"IMPACT OF EFFLUENT ORGANIC MATTER ON THE APPLICATION OF OZONE FOR TREATMENT OF ORGANIC CONTAMINANTS FROM WASTEWATER"

By

SARAH GONZALES

B.S., New Mexico Institute of Mining and Technology 2008

A thesis submitted to the

Faculty of Graduate School of the University of Colorado

in partial fulfillment of the requirement for the

degree of Master of Science

Department of Civil, Environmental and Architectural Engineering

2010

This thesis entitled:

Impact of Effluent Organic Matter on the Application of Ozone for Treatment of Organic Contaminants from Wastewater

Written by Sarah Gonzales

has been approved for the Department of Civil, Environmental and Architectural Engineering

Fernando Rosario-Ortiz (Committee Chair)

JoAnn Silverstein (Committee Member)

Karl Linden (Committee Member)

Date

The final copy of this thesis has been examined by the signatories, and we find that both the content and form meet acceptable presentation standards of scholarly work in the above mentioned discipline

ABSTRACT

Sarah Gonzales (M.S. Civil (Environmental) Engineering; Department of Civil, Environmental and Architectural Engineering)

"IMPACT OF EFFLUENT ORGANIC MATTER ON THE APPLICATION OF OZONE FOR TREATMENT OF ORGANIC CONTAMINANTS FROM WASTEWATER"

Thesis directed by Professor Fernando Rosario-Ortiz

The application of ozone for the advanced treatment of wastewater effluents is currently being evaluated throughout the world. Application of ozone to wastewater results in disinfection and significant oxidation of emerging contaminants of concern, including pharmaceuticals and personal care products. The impact of wastewater derived effluent organic matter (EfOM) on the application of ozone for the oxidation of organic contaminants was evaluated for four wastewaters (sites A, B, C1 and C2). Specifically, the ozone decomposition and concurrent formation of hydroxyl radical ($HO^{\bullet}$) from EfOM as a function of apparent molecular weight (AMW). Each collected water was fractionated into four fractions (< 10 kDa, < 5 kDa, < 3 kDa, and < 1 kDa) and characterized in terms of chemical and physical properties. The R_{CT}, defined as the ratio of $HO^{\bullet}$ exposure to ozone exposure ($\int HO^{\bullet}dt$ / $\int O_3 dt$), was measured for all fractions and bulk waters, with an initial ozone dose equal to the total concentration of EfOM. The R_{CT} of all the waters and pseudo first order decay rates of two of the waters increased significantly (95% confidence) from the bulk sample to the < 10 kDa fraction. The formation of $HO^{\bullet}$ was modeled for the C1 and C2 waters and fractions. The model showed that < 3% of the $HO^{\bullet}$ formation was attributed to the organic matter with AMW >10 kDa for the C1 water and < 18% of the $HO^{\bullet}$ formation for the C2 water. This demonstrated that the organic matter with AMW > 10 kDa was relative unreactive towards ozone as well as being a relative insignificant source of $HO^{\bullet}$. Coagulation was investigated as a pretreatment step to increase the pharmaceutical removal efficiency of the wastewaters with ozone via jar tests. The coagulated water showed a dramatic increase in the ozone pseudo-first order decay rate as well as the R_{CT}. Contaminant oxidation was also preformed on the C2 samples. The coagulated water showed greater contaminant removal than the bulk sample. The results help support the hypothesis that EfOM plays the dominant role in ozone decomposition throughout the reaction.

DEDICATIONS

This dissertation is dedicated to my parents Dr. Regina Griego and Gregory Gonzales for their constant love, support and encouragement throughout my life.

ACKNOWLEDGMENTS

I would like to express my sincere appreciation to my adviser and mentor, Dr. Fernando Rosario-Ortiz, for his guidance, intelligence, insight, generosity and patience throughout my research work. I would like to thank the Department of Civil, Environmental and Architectural Engineering from the University of Colorado for their financial support for this research project. I also thank my dissertation committee members, Professor JoAnn Silverstein and Professor Karl Linden, who have generously provided their time and valuable suggestions to my dissertation. I would like to thank to Vivy Mei Mei Dong, a doctoral student who helped me with the analytical aspects of my research. I would like to extend my appreciation to Andria Pena, an undergraduate student at the University of Puerto Rico for assisting me with my experiments and was funded courtesy of the Summer Multicultural Access to Research Training (SMART) program. I would like to extend my gratitude to Eric Wert at the Southern Nevada Water Authority for assisting in the contaminant analysis portion of my research. I would like to thank undergraduate student Garrett McKay and Professor Steve Mezyk at California State University, Long Beach for running the EfOM scavenging experiments. I would like to extend my appreciation to post doctorate student Dr. Aaron Dotson for his continued assistance and valuable suggestions in the laboratory. I would like to extend my warmest gratitude to my mother, Dr. Regina Griego, and father Gregory Gonzales for their unconditional love, patience, sacrifice and encouragement throughout my life. A special thanks to my sister, Veronica Gonzales, and brother, Matthew Gonzales, for their love and support.

TABLE OF CONTENTS

LIST OF TABLES

LIST OF FIGURES

CHAPTER 1. INTRODUCTION

1.1: Motivation

The availability of potable water has become a worldwide issue for purpose of drinking water. Increased water demands from population growth combined with the decline in source water quality have increased interest in water reuse as a means of augmenting deteriorating water supplies. Wastewater has been identified as a viable source to augment water supplies. Wastewater is unique due to its constancy as a water source that is not subject to seasonal flows, as well as being located where the greatest demand from the population are. However, there is concern with the reuse of wastewater including the required remediation of chemical and biological contamination.

Recent advances in the quantification of organic compounds has led to the widespread detection of emerging contaminants such as endocrine disrupting compounds (EDCs), pharmaceuticals and personal care products (PPCPs) and pesticides in many different fresh water sources in the parts per trillion (ppt) level (Snyder, Vanderford et al. 2003; Snyder, Westerhoff et al. 2003). A majority of these chemicals are consumed by humans for the prevention, control and cure of disease. These compounds are not fully digested and end up in the influent of a wastewater treatment plant. Because the traditional wastewater treatment processes do not fully remove these trace organics, the more recalcitrant compounds are discharged into the receiving body and find their way into downstream drinking water intakes (Snyder, Westerhoff et al. 2003). In industrialized countries more than 90% of wastewater is treated in a centralized

wastewater treatment plant (WWTP) making them a major point source for trace organic contaminants as well as the most efficient location for mitigation (Hollender 2009).

The impact of the presence of these compounds is not fully understood. Studies have shown that a few trace organic compounds such as butylbenzyl phthalate (BBP), di-n-butylphthalate (DBP) and BHA have the potential for endocrine disrupting effects (Jobling 1995). Continuing studies into the EDC compounds found examples of widespread sexual disruption of wild vertebrate populations indicating that even at ambient concentrations there is a potential to affect the ecosystem (Jobling, Nolan et al. 1998).

Research into the toxicological effects of trace organic contaminants on human physiology continues to clarify the significance of their presence in drinking water supplies. A recent study investigated the health significance of trace levels of 15 pharmaceutically active contaminants and 4 metabolites. These compounds were selected based on their level of occurrence, rate of use and potential for toxicity and were compared at concentrations detected in drinking water treatment plants. Based on animal toxicity data, screening levels were calculated for drinking water equivalent levels (DWELs). The study showed that the ratio of maximum detected concentration to DWEL of the contaminants ranged from 110 to 6,000,000. This indicates that there are no adverse human health affects expected from the targeted pharmaceuticals in US drinking water (Bruce 2010).

Public concern is the main driving force and has increased regulatory focus on the issue of EDC/PPCP presence even at the low reported levels of contamination (Snyder, Vanderford et al. 2003; Snyder, Westerhoff et al. 2003). To date, atrazine has become an

EPA regulated compound under the National Primary Drinking Water Regulations (NPDWR) with a maximum contamination level (MCL) of 0.003 mg/L (40 CFR 141.61). Other trace organic contaminants such as 17α-ethynylestradiol, 17β-estradiol, estrone and butylated hydroxyanisole (BHA) have been placed on the EPA Contaminant Candidate List (CCL3) as compounds under investigation for regulation.

Given the low level of occurrence of trace organic compounds, their removal can be challenging. Various methods of treatment have been investigated for the removal of these contaminants including physical separation such as membrane treatment or GAC adsorption (Snyder, Adham et al. 2007) and chemical oxidation through an advanced oxidation process (AOP) (Ruiz-Haas, Cho et al.; Huber, Canonica et al. 2003; Rosenfeldt and Linden 2004; Esplugas, Bila et al. 2007). An AOP is based on the increased formation of the hydroxyl radical ($HO^{\bullet}$). The $HO^{\bullet}$ is a powerful oxidant that reacts rapidly with a wide variety of organic and inorganic compounds (Buxton, Greenstock et al. 1988; von Gunten 2003). There are many types of AOPs, including ultra-violet/hydrogen peroxide (UV/H_2O_2), Photo-Fenton process, and ozone. Due to the high reactivity and scavenging capacity of the $HO^{\bullet}$ it is present in very low concentrations of $<10^{-12}$ M in most AOPs and up to $>10^{-10}$ for the initial reactions of ozone AOP in wastewater (Buffle, 2006).

1.2: Application of Ozone for Contaminant Oxidation

AOPs have been shown to be very effective at the removal of numerous trace organic contaminants from drinking water and wastewater (Huber, 2003; Hollender, 2009; Snyder, 2006; Wert, 2009; Rosario-Ortiz, 2009). For example, ozone reacts either

directly with a compound or through its degradation product, $HO^{\bullet}$. Both of these oxidants are contributors in the oxidation of trace organic contaminants (Xiong, 1992; Westerhoff, 1997; Elovitz, 1999; Snyder, 2007; Rosario-Ortiz, 2009). Ozone is a very selective oxidant with a second order reaction rate ranging over several orders of magnitude from 0.75 $M^{-1}s^{-1}$ for diazepam to $2.5x10^{6}$ $M^{-1}s^{-1}$ for sulfamethoxazole (Huber, Canonica et al. 2003). The $HO^{\bullet}$ is an unselective oxidant that reacts with reported second order rate constants between 10^{8}-10^{10} $M^{-1}s^{-1}$ for many trace organic contaminants (Buxton, Greenstock et al. 1988). In a comparison study of UV/H_2O_2 against ozone AOP it was reported that the energy required to form $HO^{\bullet}$ for several distinct surface waters was less for ozone making it the more efficient AOP for the majority of the tested waters (Rosenfeldt and Linden 2004; Rosenfeldt, Linden et al. 2006).

The molecular structure of ozone causes it to be highly unstable in water and extremely reactive. This high reactivity is attributed to the electronic configuration of the molecule. Figure 1.1 illustrates the various structures of the ozone molecule.

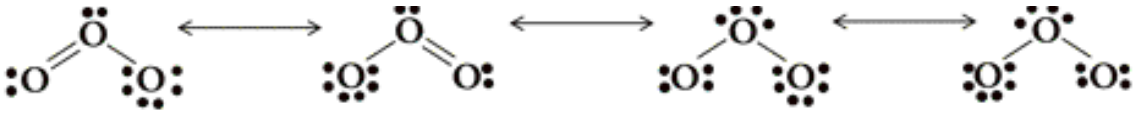

Figure 1.1: Structure of the ozone molecule and the four canonical forms.

The absence of electrons from one end of the terminal oxygen atoms gives ozone a very strong electrophilic character (Beltran 2004). In opposition to the electrophilic character of the positive terminal oxygen, the excess negative charge on one of the other oxygen atoms gives ozone a nucleophilic character as well (Beltran 2004).

There are two main mechanisms for the reaction of ozone with organic compounds. The first is a cycloaddition reaction where ozone targets the carbon-carbon double bond (C=C) such as olefinic compounds (Beltran 2004). The most well-known cycloaddition mechanism is the Criegge mechanism (Figure 1.2). The Criegge mechanism occurs when ozone forms an unstable five-member ring or ozonide.

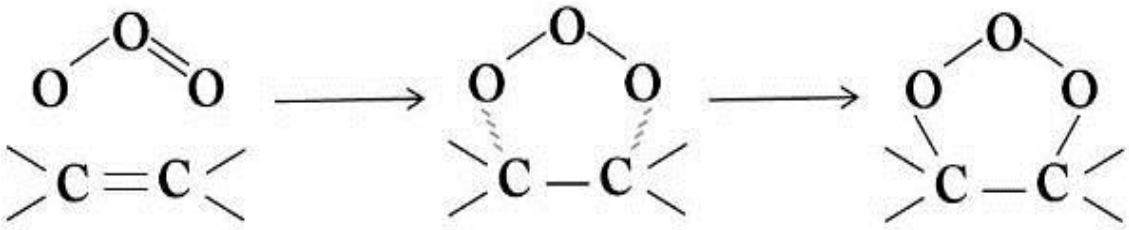

Figure 1.2: Ozonide Ring formed by the Criegge Mechanism.

The ozonide reacts in a variety of ways that could produce another ozonide, peroxide or keytone. The completion of the reaction results in the formation of keytones, aldehydes or acids. Ozone could also react with aromatic compounds through 1,3-cycloaddition reactions resulting in the breakup of the aromatic ring (Beltran 2004). However, cycloaddition reactions are less probable in aromatic compounds than an electrophilic attack of the terminal oxygen of ozone on a nucleophilic center of the aromatic compound (Beltran 2004).

The second mechanism is electrophilic substitution reactions. Electrophilic substitution is when ozone attacks one nucleophilic position on the organic compound resulting in the substitution of one part of the molecule. This reaction is the basis of ozone reactions with aromatic compounds such as phenols. Aromatic compounds are more likely to undergo electrophilic substitution rather than cycloaddition due to the

stability of the aromatic ring structure. Unlike cycloaddition, electrophilic substitution does not lead to the break up of the ring structure, only the loss of aromaticity. These reactions result in the formation of $HO^{\bullet}$ (Beltran 2004).

1.2.1: Ozone Decomposition in Water

Numerous investigations have been conducted on the decomposition of ozone in pure water. The first model was proposed in 1935 and since then there have been two models that were accepted as of 2004, however; further studies are ongoing (Weiss 1935; Sonntag and Schuchmann 1994). The model of Staehelin, Hoigne and Buhler (SHB) is used in low to neutral pH ranges. (Staehelin and Hoigne 1982; Buhler, Staehelin et al. 1984; Staehelin, Buhler et al. 1984; Tomiyasu, Fukutomi et al. 1985; Sonntag and Schuchmann 1994). The SHB model is more widely used since most systems have a more neutral pH. This model consists of a series of initiation, propagation and termination reactions as shown in Table 1.1.

Table 1.1: The SHB Ozone Decomposition Mechanism in Pure Water

Initiation Re*action*:		
$O_3 + OH^- \xrightarrow{k_1} HO_2\bullet + O_2^-\bullet$	$k_1 = 70 M^{-1}s^{-1}$	(1.1)
Pr*opogation* Re*actions*:		
$HO_2\bullet \xrightarrow{k_2} O_2^-\bullet + H^+$	$k_2 = 7.9\times10^5 \text{ sec}^{-1}$	(1.2)
$O_2^-\bullet + H^+ \xrightarrow{k_3} HO_2\bullet$	$k_3 = 5\times10^{10} M^{-1}s^{-1}$	(1.3)
$O_3 + O_2^-\bullet \xrightarrow{k_4} O_3^-\bullet + O_2$	$k_4 = 1.6\times10^9 M^{-1}s^{-1}$	(1.4)
$O_3^-\bullet + H^+ \xrightarrow{k_5} HO_3\bullet$	$k_5 = 5.2\times10^{10} M^{-1}s^{-1}$	(1.5)
$HO_3\bullet \xrightarrow{k_6} HO\bullet + O_2$	$k_6 = 1.1\times10^5 \text{ sec}^{-1}$	(1.6)
$O_3 + HO\bullet \xrightarrow{k_7} HO_4\bullet$	$k_7 = 2\times10^9 \text{ sec}^{-1}$	(1.7)
$HO_4\bullet \xrightarrow{k_8} HO_2\bullet + O_2$	$k_8 = 2.8\times10^4 \text{ sec}^{-1}$	(1.8)
*Ter*min*ation* Re*actions*:		
$HO_4\bullet + HO_4\bullet \xrightarrow{k_9} H_2O_2\bullet + O_3$	$k_9 = 5\times10^9 M^{-1}s^{-1}$	(1.9)
$HO_4\bullet + HO_3\bullet \xrightarrow{k_{10}} H_2O_2\bullet + O_2 + O_3$	$k_{10} = 5\times10^9 M^{-1}s^{-1}$	(1.10)

The initiation reaction in pure water is between ozone and the hydroxide ion forming the superoxide ion. Increasing the pH of the system will increase OH^- concentrations and accelerate ozone decay. The formation of the superoxide ion radical is key in the propagation of radical species. The superoxide radical will rapidly react with ozone and other radical species leading to the formation of the $HO^\bullet$. Finally there are the termination reactions of ozone decomposition. These are the species that react with $HO^\bullet$ but do not yield products that propagate its formation. These species are referred to as inhibitors (Beltran 2004).

The model of Tomiyasu, Fukutomi and Gordon (TFG) is more representative at high pH ranges and is not as widely used as the SHB model (Tomiyasu, Fukutomi et al. 1985) (see Table 1.2). Like the SHB model, the TFG model describes the initiation reaction with OH^- followed by a series of propagation reactions ending with termination reactions. Unlike the SHB model, the TFG model assumes the solution is slightly

alkaline and that carbonate species are available. These carbonate species are shown to be inhibitors in the formation of $HO^{\bullet}$.

Table 1.2: TFG Ozone Decomposition Mechanism in Pure Water with Alkalinity

Initiation Reaction:		
$O_3 + OH^- \xrightarrow{k_{11}} HO_2\bullet + O_2^-\bullet$	$k_{11} = 40 M^{-1}s^{-1}$	(1.11)
$HO_2\bullet \xrightarrow{k_{12}} O_2^-\bullet + H^+$	$k_{12} = 2.2\times10^6 M^{-1}s^{-1}$	(1.12)
Propogation Reactions:		
$HO_2\bullet \xrightarrow{k_{13}} O_2^-\bullet + H^+$	$k_{13} = 7.9\times10^5 M^{-1}s^{-1}$	(1.13)
$O_2^-\bullet + H^+ \xrightarrow{k_{14}} HO_2\bullet$	$k_{14} = 5\times10^{10} M^{-1}s^{-1}$	(1.14)
$O_3^-\bullet + O_2^-\bullet \xrightarrow{k_{15}} O_3^-\bullet + O_2$	$k_{15} = 1.6\times10^9 M^{-1}s^{-1}$	(1.15)
$O_3^-\bullet + H_2O \xrightarrow{k_{16}} HO\bullet + O_2 + OH^-$	$k_{16} = 20-30 M^{-1}s^{-1}$	(1.16)
$O_3\bullet + HO\bullet \xrightarrow{k_{17}} HO_2\bullet + O_2^-\bullet$	$k_{17} = 6\times10^9 M^{-1}s^{-1}$	(1.17)
$O_3 + HO\bullet \xrightarrow{k_{18}} HO_2\bullet + O$	$k_{18} = 3\times10^9\ \text{sec}^{-1}$	(1.18)
$HO_2^- + H^+ \xrightarrow{k_{19}} H_2O_2$	$k_{19} = 5\times10^{10}\ \text{sec}^{-1}$	(1.19)
$H_2O_2 \xrightarrow{k_{20}} HO_2^- + H^+$	$k_{20} = 0.25\ \text{sec}^{-1}$	(1.20)
Termination Reactions:		
$O_3 + HO\bullet \xrightarrow{k_{21}} O_3 + OH^-$	$k_{21} = 2.5\times10^9 M^{-1}s^{-1}$	(1.21)
$HO\bullet + CO_3 \xrightarrow{k_{22}} OH^- + CO_3^-\bullet$	$k_{22} = 4.2\times10^8 M^{-1}s^{-1}$	(1.22)
$CO_3^-\bullet + O_3 \xrightarrow{k_{23}} O_2 + CO_2 + O_2^-\bullet$	*NA*	(1.23)

1.2.2: Ozone Decomposition in the Presence of Organic Matter

In the presence of organic matter, the HO^- pathway no longer dominates. DOM becomes the preferred pathway due to the faster kinetics. DOM acts as both a scavenger and a promoter in the system. As a promoter DOM reacts with ozone in two ways, direct reactions with ozone through electron transfer to form a superoxide radical or reactions with $HO^{\bullet}$ to form a carbon centered radical (Hoigne 1998). The reaction of the carbon-centered radical with oxygen will lead to the formation of superoxide radical which will

lead to the formation of $HO^{\bullet}$ (von Gunten 2007). The propagation effect with DOM and $HO^{\bullet}$ is as follows:

$$^{\bullet}HO + DOM \rightarrow DOM^{\bullet} + H_2O \; or \; DOM^{\bullet} - OH \quad (1.24)$$

$$DOM^{\bullet} + O_2 \rightarrow DOM - O_2^{\bullet} \rightarrow DOM^{+} + O_2^{\bullet -} \quad (1.25)$$

DOM can also react directly with the $HO^{\bullet}$ acting as a scavenger by not producing the carbon centered radical and thereby terminating the reaction.

$$^{\bullet}HO + DOM \rightarrow DOM_{ox} + H_2O \quad (1.26)$$

The decay of ozone in natural waters has been characterized by an initial and second phase. In the initial phase (times less than 20 seconds), the ozone decay follows an exponential function (Buffle, Schumacher et al. 2006). The second phase (t > ~20 seconds) has a much slower ozone decay that is modeled as pseudo first-order decay (Elovitz and von Gunten 1999; Buffle, Schumacher et al. 2006; Buffle, Schumacher et al. 2006). The two mechanisms for ozone decay are the reaction of ozone and pure water, more specifically OH^-, and the reaction of ozone with DOM. The initial phase consists of the DOM reaction pathway. Ozone has a high reactivity with specific DOM moieties such as secondary and tertiary amines, and phenols (Buffle and Von Gunten 2006). The second phase occurs when all the rapid reacting DOM moieties have been oxidized and the HO^- pathway becomes preferred. In the second phase ozone reacts with HO^- to form peroxide, which continues to form radical species until $HO^{\bullet}$ is produced. Figure 1.3 illustrates the DOM and OH^- ozone decomposition pathways.

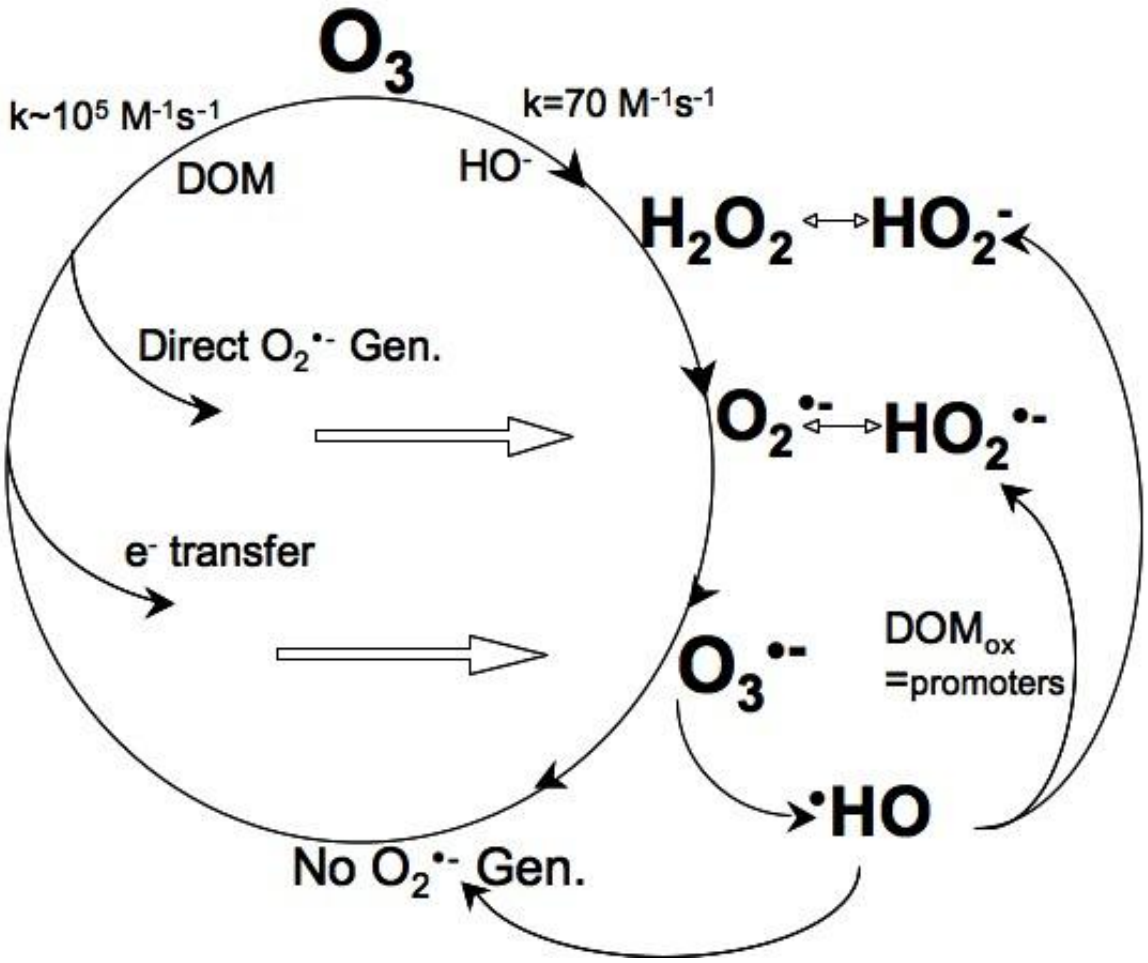

Figure 1.3: Ozone Decomposition Pathways. During the initial phase certain DOM moieties will react directly with ozone to form $O_2^{\bullet -}$ or via direct electron transfer. During the second phase specific DOM moieties will promote ozone decomposition.

1.3: Effluent Organic Matter

Wastewater EfOM is composed of background natural DOM as well as soluble microbial products (SMPs) that are generated in the wastewater treatment process. Natural water sources contain microbial and terrestrially derived organic matter (Krasner, Croue et al. 1996). During traditional drinking water treatment some of the organic

matter is removed but the remaining recalcitrant fraction is conveyed through the home and eventually into the wastewater stream.

SMP are divided into two categories and are composed of a variety of complex organic compounds including proteins, polysaccharides, humic material, and organic acids (Pribyl 1997). The first category is biomass-associated products (BAP) and the second is utilization-associated products (UAP) (Namkung and Rittmann 1986). BAP are created from cellular decay and have a positive correlation with the biomass concentration in an activated sludge process. The UAP are connected to cellular metabolism and biomass production and as such is connected with substrate utilization and cellular growth. The AMW distribution of SMP varies widely from <0.5 kDa to >100 kDa. The UAP are on the lower molecular weight end of the distribution, with an AMW of <1 kDa and the BAP are on the large end of the molecular weight distribution with a AMW of approximately >10 kDa (Boero 1996; Jiang 2010).

1.4: Ozone in Wastewater

Studies into the ozonation of wastewater looked at the effect of ozone dose, organic matter and $HO^{\bullet}$ scavengers on the decomposition and generation of $HO^{\bullet}$ (Buffle, Schumacher et al. 2006). This study demonstrated the importance of EfOM on the ozone decay and $HO^{\bullet}$ generation. The study observed a difference in the ozone reaction kinetics for the wastewater systems when compared to natural water systems. In surface waters, the reactive moieties of DOM are consumed during the initial phase of ozone decomposition; in wastewater, the high concentrations of EfOM make it an important promoter/scavenger throughout the ozone decomposition. The higher EfOM

concentrations also require higher ozone doses. Natural water systems display the two-phase ozone decomposition profile described in Section 1.2, however; wastewater systems have kinetics similar to the initial phase throughout the process. This behavior indicates that reactions with EfOM dominate the ozone decomposition (Buffle, Schumacher et al. 2006). Since EfOM plays such a dominant role in the decomposition of ozone, it would be beneficial to understand and model both the promotion and scavenging. The $HO^{\bullet}$ scavenging capacity of EfOM can be studied independently from ozone using electron pulse radiolysis (Rosario-Ortiz 2004; Rosario-Ortiz, Mezyk et al. 2008; Dong 2010). This is the first study to examine the $HO^{\bullet}$ promotion and formation capacity of EfOM.

1.5: Modeling Contaminant Removal during Ozonation of Wastewater

Contaminants are oxidized either by ozone, $HO^{\bullet}$ or both. Due to the difficulty of measuring $HO^{\bullet}$, Elovitz and von Gunten developed a relationship for estimating the $HO^{\bullet}$ concentration in a natural system. The R_{CT} is defined as the ratio between $HO^{\bullet}$ and ozone exposure ($R_{CT} = \int HO^{\bullet}dt / \int O_3 dt$) (Elovitz and von Gunten 1999). In natural waters the R_{CT} variation can be fitted by a power function during the initial phase but is constant during the second phase of ozone decomposition. In a water utility, samples are taken in the second and minute time frame so the constancy of the R_{CT} in the this time frame makes it a good tool and simplification of modeling ozone and $HO^{\bullet}$ exposures as well as contaminant removal in natural waters.

A study looking at the R_{CT} in wastewater examined the ozone and $HO^{\bullet}$ exposures in initial phase more closely using the continuous quench–flow system (CQFS) (Buffle,

Schumacher et al. 2006). The CQFS study was used to examine the first 20 seconds of ozone decomposition kinetics. The study found that in the first 20 seconds of ozone exposure there are very high $HO^{\bullet}$ to ozone exposures and high R_{CT} (~10^{-6}). These high radical exposure ratios showed that the ozonation of wastewater generates enough $HO^{\bullet}$ to be considered an AOP. This study found that for wastewaters the R_{CT} was not constant throughout the entire reaction making it less accurate for system modeling.

The effects of ozone exposure on the oxidation of organic contaminants were investigated for three wastewaters (Wert, Rosario-Ortiz et al. 2009). The impact of wastewater quality (EfOM, alkalinity, nitrite, etc.) on ozone decomposition was examined for the removal of 31 trace organic contaminants. It was found that wastewaters with larger molecular weight components had increased ozone decomposition when compared on a normalized TOC basis. For contaminant removal, this study found that the compounds with high ozone reactivity ($k_{O3} > 10^5$ $M^{-1}s^{-1}$) were well removed independent of water quality, however; compounds with limited ozone reactivity ($k_{O3} < 10$ $M^{-1}s^{-1}$) varied with wastewater quality and were dependent on the compound specific reactivity with $HO^{\bullet}$ (k_{HO}). In this study, one of the waters behaved contrary to the other two for an O_3/H_2O_2 AOP process. Two of the wastewaters showed accelerated $HO^{\bullet}$ production whereas one of the waters showed a marked decrease in $HO^{\bullet}$ exposure. This result indicates that wastewater quality has a significant impact on the system reaction kinetics.

1.6: Scope of Study

EfOM dominates the reactions of ozone in wastewater throughout the ozonation process because of high EfOM concentrations and the higher ozone dose required for oxidation (Buffle, Schumacher et al. 2006). EfOM plays an important role as both a promoter and scavenger of $HO^{\bullet}$ in the reactions with ozone. Previous research has investigated the $HO^{\bullet}$ scavenging capacities of EfOM and empirical models have been developed to infer the $HO^{\bullet}$ concentration in an ozonated wastewater system, however; the role of EfOM on the $HO^{\bullet}$ promotion and formation capacity has not been investigated. The studies conducted in this thesis examine the impact of the molecular weight distribution of EfOM on the $HO^{\bullet}$ formation capacity of the wastewater. A better understanding of the $HO^{\bullet}$ formation capacity of EfOM as a function of AMW will allow better understanding of ozone in wastewater. Looking at the AMW of wastewater specifically as a function of wastewater treatment makes it possible to optimize the treatment process for ozone AOP and contaminant removal.

CHAPTER 2. HYPOTHESIS AND OBJECTIVES

The main objective for this work was to understand the formation role of EfOM on the decay of ozone and formation of $HO^{\bullet}$. Previous work investigated the overall scavenging of $HO^{\bullet}$ by EfOM as a function of AMW in order to understand how specific components of this mixture impact $HO^{\bullet}$ concentrations (Dong 2010). This work looked into how EfOM impacted ozone decay and $HO^{\bullet}$ formation. By understanding $HO^{\bullet}$ formation, a better understanding of ozone in wastewater can be obtained, especially looking at the role of wastewater processes on the properties of EfOM. Increased understanding of the influence of wastewater process on ozone reactions will allow for the optimization of wastewater treatment for trace organic contaminant oxidation.

This work evaluated three main hypotheses:

Hypothesis 1: The molecular composition of EfOM will dictate its role as a promoter/scavenger.

Previous studies into the R_{CT} of wastewater ozonation showed that the R_{CT} and $HO^{\bullet}$-exposures are very high and exhibit exponential decay throughout the reaction. These results for the ozone decomposition kinetics suggest that the main mechanism of ozone decomposition in wastewater is the direct reaction with specific EfOM moieties (Buffle, Schumacher et al. 2006). Therefore, a better understanding of which EfOM components have the greatest influence over $HO^{\bullet}$ promotion and scavenging will allow

for the potential optimization of wastewater processes for the formation of $HO^{\bullet}$ for contaminant removal in ozone AOP.

Hypothesis 2: EfOM from different wastewater treatment processes will behave differently.

Wastewater EfOM is dependant on the recalcitrant DOM in the drinking water as well as SMP generated at the wastewater treatment plant. A previous study into the $HO^{\bullet}$ reaction rate constant of wastewater shows that EfOM from different treatment plants display a wide range of characterization parameters (TOC, UV_{254}, SUVA, FI, etc.) as well as reaction kinetics (Rosario-Ortiz, Mezyk et al. 2008). These differences in wastewater characterization affect the reaction kinetics with ozone.

CHAPTER 3. MATERIALS AND METHODS

3.1: Sample Collection

Four samples were collected at three wastewater treatment facilities (A, B, C1 and C2) in the United States. Sites A and B utilized activated sludge (A/S) with nitrification/dinitrification. However, site A utilized aerobic and anoxic conditions and did not achieve full nitrification/denitrification while site B used anaerobic condition in addition to the aerobic and anoxic conditions and attained complete nitrification/denitrification. Two other samples were collected at one facility that had two different treatment trains (site C). Site C1 used partial nitrification/dinitrification A/S and site C2 used A/S without nitrification. The samples were collected prior to final disinfection. Once received, the samples were filtered through 0.7 μm glass fiber filters and stored at 4 °C until analyzed. Samples were analyzed within two weeks of collection.

3.2: EfOM Fractionation

The method for EfOM fractionation employed by Dong et al. 2010 was used. In this method, sample fractionation was achieved utilizing ultra-filtration (UF), with a modified version of a previously established method (Revchuk, 2009 #1). Four membranes (YM 1, 3, 5, and 10 kDa) obtained from Millipore (Millipore, MA, USA) and a solvent resistant stir cell (Model XFUF 07601, Millipore, MA, USA) were used for this study. The membranes were first soaked in 1L of Milli-Q water (resistance = 18.2 MΩ·cm), with three water changes before use. Any remaining glycerin preservative was removed by passing 200 mL of Milli-Q water through the membrane under 75psi N_2 of

constant pressure. The first 120 mL of the filtrate was wasted, while the remaining 80 mL collected was used to measure the background carbon concentration. The UF membrane did not affect the concentration of inorganic species (Dong 2010). Table 3.1 demonstrates that the pretreatment process for the UF membranes removed the remaining glycerin preservative.

Table 3.1: Background DOC for < 10, < 5, < 3 kDa Ultrafiltration membrane as a function of volume of water throughput.

Volume (mL)	DOC (mg/L)					
	10K I	10K II	5K I	5K II	3K I	3K II
20	0.78	0.42	0.78	0.25	0.55	2.64
35	0.11	0.21	0.13	0.14	0.26	0.60
50	0.07	0.06	0.10	0.12	0.25	0.48
65	0.04	0.07	0.07	0.10	0.17	0.37
80	0.03	0.05	0.08	0.09	0.29	0.28
95	0.03	0.06	0.05	0.08	0.18	0.19
110	0.06	0.05	0.03	0.08	0.19	0.21
125	0.03	0.05	0.02	0.07	0.15	0.17
140	0.02	0.05	0.02	0.10	0.14	0.14
155	0.01	0.06	0.16	0.07	0.15	0.18
170	0.01	0.05	0.21	0.07	0.23	0.16
185	0.02	0.07	0.03	0.08	0.20	0.16
200	0.09	0.11	0.02	0.17	0.19	0.28
215	0.03	0.04	0.09	0.07	0.12	0.27
230	<DL	<DL	<DL	0.01	0.16	0.26
245	<DL	<DL	<DL	0.59	0.15	0.05
260	<DL	<DL	<DL	0.09	0.11	0.16
275	<DL	<DL	<DL	<DL	0.10	0.27
290	<DL	<DL	<DL	<DL	0.09	0.06
300	<DL	<DL	<DL	<DL	0.24	0.10

3.3: Analytical Methodology.

DOC (minimum detection level (MDL) = 0.2 mg_C/L) and total dissolved nitrogen (TN) (MDL = 0.040 mg_N/L) were measured using a TOC-V_{SCH} (Shimadzu Corp., Japan) analyzer. Nitrate (NO_3^-) (MDL = 0.010 mg_N/L) and nitrite (MDL = 0.010 mg_N/L) were

determined using ion chromatography (IC) (DX-500 Dionex Corp., CA, USA) following standard methods (APHA, 2005 #796). IC samples were filtered though Ag/H cartridges (On Guard II, Dionex Corp., CA, USA) to remove excess chloride prior to analysis. Ammonia (MDL = 0.015 mg_N/L) was measured with method TNT-830 using Hach DR-5000 (Hach Corp., USA). Alkalinity, ultra-violet absorbance at 254nm (UV_{254}) and pH were measured using standard procedures (APHA, 2005 #796). The $HO^{\bullet}$ probe compound parachlorobenzoic acid (pCBA) was quantified using an Agilent 1200 series HPLC. Samples were run with a methanol/phosphoric acid buffer gradient starting at 60% methanol, changing to 100% methanol and back to 60%. The Minimum reporting limit (MRL) for pCBA was 5µg/L.

3.4: EfOM Characterization.

Molecular weight characterization was performed using size exclusion chromatography (Fonseca, Summers et al.) with UV_{254} and DOC quantification according to the conditions described elsewhere (Her, Amy et al. 2002; Dong 2010). An Agilent 1200 LC system (Palo Alto, CA, USA) with a Toyopearl HW-50 S 250 x 20 mm column (Chromatography, Rottenburg, Germany) was used with an injection volume of 2.0 mL. The detector consisted of a diode array from Agilent (Model 1200 Palo Alto, CA, USA) monitoring at a wavelength of 254 nm. The mobile phase consisted of a phosphate buffer (0.0024 M NaH_2PO_4, 0.0016 M Na_2HPO_4 and 0.025 M Na_2SO_4) adjusted to pH 6.8 ± 0.1. The flow rate was operated at 1.0 mL/min. A modified commercially available Sievers-800 total organic carbon (TOC) analyzer (General Electric, CO, USA) with 2.0 µL/min acid and oxidizer flow rate was used to monitor the DOC elution from the SEC column.

An Agilent interface (model 35900e Palo Alto, CA, USA) was used to record voltage output from the TOC. The voltage output was linearly correlated to TOC analyzer signal. Polyethylene glycols (Arbuckle, Hrudey et al.) (Fluka, Milwaukee, WI, USA) were used for calibration and estimation of average AMW. The AMW values are presented in Daltons.

Florescence index was determined for each sample using an LS55 PerkinElmer as the ratio of emission wavelengths 450/500 nm at an excitation wavelength of 370 nm (McKnight D.M 2001). The UV_{254} absorbance was taken on a HACH 5000.

3.5: Ozonation at Bench Scale

Bench-scale tests were performed using a batch reactor to obtain information about ozone decomposition and $HO^{\bullet}$ exposure. Milli-Q water was placed inside a water-jacketed flask and cooled to 4°C. Once cooled, gaseous ozone was diffused into the water using an oxygen-fed generator to generate ozone stock solution (WEDCO GSO). Ozone stock solution concentrations were typically between 65-70 mg/L. Ozone doses were applied by injecting an aliquot of the stock solution into a 50 mL glass beaker containing 25 mL of sample.

Ozone doses were calculated to account for both inorganic and organic ozone decomposition pathways. The C2 wastewater contained nitrite. Nitrite reacts rapidly with ozone according to a mass ratio of approximately 1.1 mg-O_3/mg NO_2 (Wert, Rosario-Ortiz et al. 2009). Once the nitrite demand was determined, ozone:DOC mass ratio of 1.0 was used to evaluate the impact of EfOM molecular weight reactivity on

ozone and $HO^{\bullet}$ formation. The overall ozone dose transferred was a function of nitrite concentration and ozone:DOC ratio.

During the bench-scale tests, all experiments were performed at room temperature (20°C). Dissolved ozone residual samples were collected at 5, 10, 20, 30, 40, 50, 60, 120 and 300 seconds into the reaction to determine the ozone decomposition. Duplicate experiments were performed by adding 150 μg/L (0.4 μM) of pCBA to the tertiary wastewater. During these experiments, dissolved ozone residual and pCBA samples were collected at the same time intervals as the ozone decomposition tests. The degradation of pCBA throughout the ozonation process provided a measurement of $HO^{\bullet}$ exposure. Samples for pCBA analysis were quenched with a small aliquot of sodium thiosulfate ($Na_2S_2O_3$). Both ozone and pCBA decay experiments were run in triplicate to prove reproducibility of the results.

Ozone stock solution concentrations and dissolved ozone residuals were measured according to the indigo method described in Standard Methods 4500-O_3 (APHA et al., 1998, Bader and Hoigne, 1982). Potassium indigotrisulfonate (Sigma-Aldrich, St. Louis, MO USA) was used to generate indigo solutions with molar absorptivity of 20,000 $M^{-1}cm^{-1}$.

3.6: Contaminant Analysis

Contaminant analysis was performed by the Southern Nevada Water Authority research and development lab using online-solid phase extraction followed by liquid chromatography with tandem mass spectrometry (LC-MS/MS) according to the methods described by Tronholm et al. (Trenholm, Vanderford et al. 2008).

3.7: Coagulation

Preliminary jar tests were performed on the C2 sample according to the EPA 815-R-99-012 Enhanced Coagulation and Enhanced Precipitative Softening Guidance Manual. The coagulant used was ferric chloride ($FeCl_3$). The coagulant was added to one-liter containers of bulk C2 water at separate doses of 5.5, 11, and 16 mg/L (10, 20, and 30 mg/L Alum equivalent) respectively. The samples were run in rapid mix for one minute at 100 rpm and allowed to flocculate for 30 minutes at 30 rpm. Then the mixing was turned off and the samples were allowed to settle for 1 hour before being filtered by a 0.7 μm glass fiber filter.

3.8: Determination of Scavenging of $HO^{\bullet}$ by EfOM

The linear accelerator (LINAC) electron pulse radiolysis facility at the Radiation Laboratory, University of Notre Dame, was used for the quantification of the first order reaction constant between $HO^{\bullet}$ with EfOM ($k_{EfOM\text{-}HO^{\bullet}}$) for the bulk and fractionated wastewaters. The irradiation and transient adsorption detection system has been described in previous work as well as the procedure for $k_{EfOM\text{-}HO^{\bullet}}$ determination (Whitham, Lyons et al. 1995; Rosario-Ortiz, Mezyk et al. 2008).

The bulk and fractionated wastewaters were pre–saturated with N_2O gas, to ensure measurable formation of $HO^{\bullet}$ radicals when radiated. The formed $HO^{\bullet}$ rapidly reacted with the water components such as EfOM, nitrite and HCO_3^-, CO_3^{2-}. For the individual water samples, random kinetic analyses were run in duplicate, with $k_{EfOM\text{-}HO^{\bullet}}$ values well within the measurement error. The reported errors for these $k_{EfOM\text{-}HO^{\bullet}}$ values are a combination of

the measurement precision and concentration errors. During these $k_{EfOM\text{-}HO\bullet}$ measurements, the solution vessel was continuously sparged with the minimum concentration of N_2O necessary to prevent air ingress. Dosimetry was performed using N_2O–saturated, 1.00×10^{-2} M KSCN solutions at $\lambda = 475$ nm, ($G\varepsilon = 5.2 \times 10^{-4}$ m^2 J^{-1}) with average doses of 3-5 Gy per 3-4 ns pulse (Buxton, 1995 #2).

CHAPTER 4. OZONE DECOMPOSITION IN WASTEWATER

4.1: Sample Characterization and General Water Quality

The general water quality characteristics for sample sites A, B, C1 and C2 are presented in Table 4.1. The waters had a DOC ranging from 5.5 – 11.7 mg_C/L and nitrate concentrations ranged from 12.17 – 16.61 mg_N/L. Only sample C2 contained measurable nitrite. The alkalinity ranged from 93 – 221 mg/L, with sample A wastewater having the least amount of alkalinity and sample C2 having the greatest. The C1 and C2 samples were of particular interest due to the single influent and dual treatment trains giving a better understanding of the importance of the treatment process.

Table 4.1: General Water Quality Parameters for Collected Samples

Sample	DOC (mg_C/L)	NO_3 (mg_N/L)	NO_2 (mg_N/L)	Alkalinity (mg/L as $CaCO_3$)	UVA_{254}	$SUVA_{254}$	FI
A	6.2	12.17	<DL	93	0.12	2.00	2.38
B	5.5	16.61	<DL	108	0.10	1.76	2.39
C1	7.9	12.90	<DL	152	0.17	2.14	2.48
C2	11.7	16.27	0.04	221	0.17	1.43	2.51

Each sample was separated into <10, <5, <3 and <1 kDa fractions. The water quality characteristics of each fraction are presented in Table 4.2 through 4.4. The levels of inorganic nitrogen and alkalinity in the water remain constant through out each of the fractions in a given sample. There was no significant difference found in both the specific ultraviolet absorbance at 254 nm (SUVA) and fluorescence index (FI) values within the sample fractions. The cause of the constancy of the SUVA and FI values is unknown. One possible explanation is that the <1 kDa fraction, which is present in all fractions,

dominates the general water quality characteristics. For samples A, B, C1 and C2 the <1 kDa samples account for 37.1%, 43.6%, 35.4% and 30.8% of the EfOM respectively. The DOC and UV_{254} decreased with each decreasing fraction showing that a physical separation between the fractions was achieved.

Table 4.2: Water Quality for Fractionated Samples from Site A

Fraction (kDa)	DOC (mg_C/L)	UVA_{254}	$SUVA_{254}$ (m^1L/mg_C)	FI
A				
Bulk	6.2	0.12	2.00	2.38
<10	4.8	0.09	1.97	2.28
<5	3.4	0.08	2.20	2.29
<3	2.7	0.05	1.89	2.36
<1	2.3	0.04	1.96	2.37

Table 4.3: Water Quality for Fractionated Samples from Site B

Fraction (kDa)	DOC (mg_C/L)	UVA_{254}	$SUVA_{254}$ (m^1L/mg_C)	FI
B				
Bulk	5.5	0.10	1.76	2.39
<10	4.6	0.08	1.80	2.41
<5	3.7	0.07	1.76	2.44
<3	2.8	0.06	2.03	2.46
<1	2.4	0.04	1.83	2.52

Table 4.4: Water Quality for Fractionated Samples from C1 and C2 Sites

Fraction (kDa)	DOC (mg_c/L)	UVA_{254}	$SUVA_{254}$ (m^1L/mg_C)	FI
C1				
Bulk	7.9	0.17	2.15	2.48
<10	6.0	0.13	2.17	2.43
<5	4.9	0.11	2.24	NA
<3	4.1	0.09	2.19	2.43
<1	2.8	0.06	2.14	2.44
C2				
Bulk	11.7	0.17	1.45	2.51
<10	8.0	0.13	1.63	2.52
<5	5.4	0.09	1.67	2.50
<3	4.8	0.09	1.88	2.50
<1	3.6	0.07	1.94	2.50

Figures 4.1 and 4.2 illustrate the SEC for the C1 and C2 fractions (no SEC characterization was done on the A and B samples). There were three distinct peaks on the DOC response curve. The first large peak corresponds to components of approximately 30 kDa in size, the second peak contains the material that is between 1 and 10 kDa and the third peak consists of the material <1 kDa in size. Material with AMW greater than 10 kDa is associated with organic colloids with low aromatic content whereas material with AMW between 1 and 10 kDa is associated with the humic-like material. Material with AMW <1 kDa are associated with hydrophilic material (Her 2003; Allpike, Heitz et al. 2005; Jarusutthirak and Amy 2007; Nam, Krasner et al. 2008; Song 2010). The large peak shown on the SEC plots in Figures 4.1 and 4.2 show a lower normalized UV_{254}/DOC ratio than the other apparent molecular weight (AMW) fractions (Song 2010). Polysaccharides have low absorbance and could make up a large portion of the colloidal organic matter. Polysaccharides consist of polymeric carbohydrate structures with repeating units joined together by glycosidic bonds. These structures are

often linear, but may contain various degrees of branching. The lower AMW fractions have a larger normalized UV_{254}/DOC ratio that characterizes the more fulvic-like and low molecular weight acids of the organic matter (Song 2010). The third peak relates to the very small AMW fractions of organic matter that have low UV_{254} absorbance characterizing the more aliphatic material. This material is comprised mostly of UAP (Boero 1996; Jiang 2010).

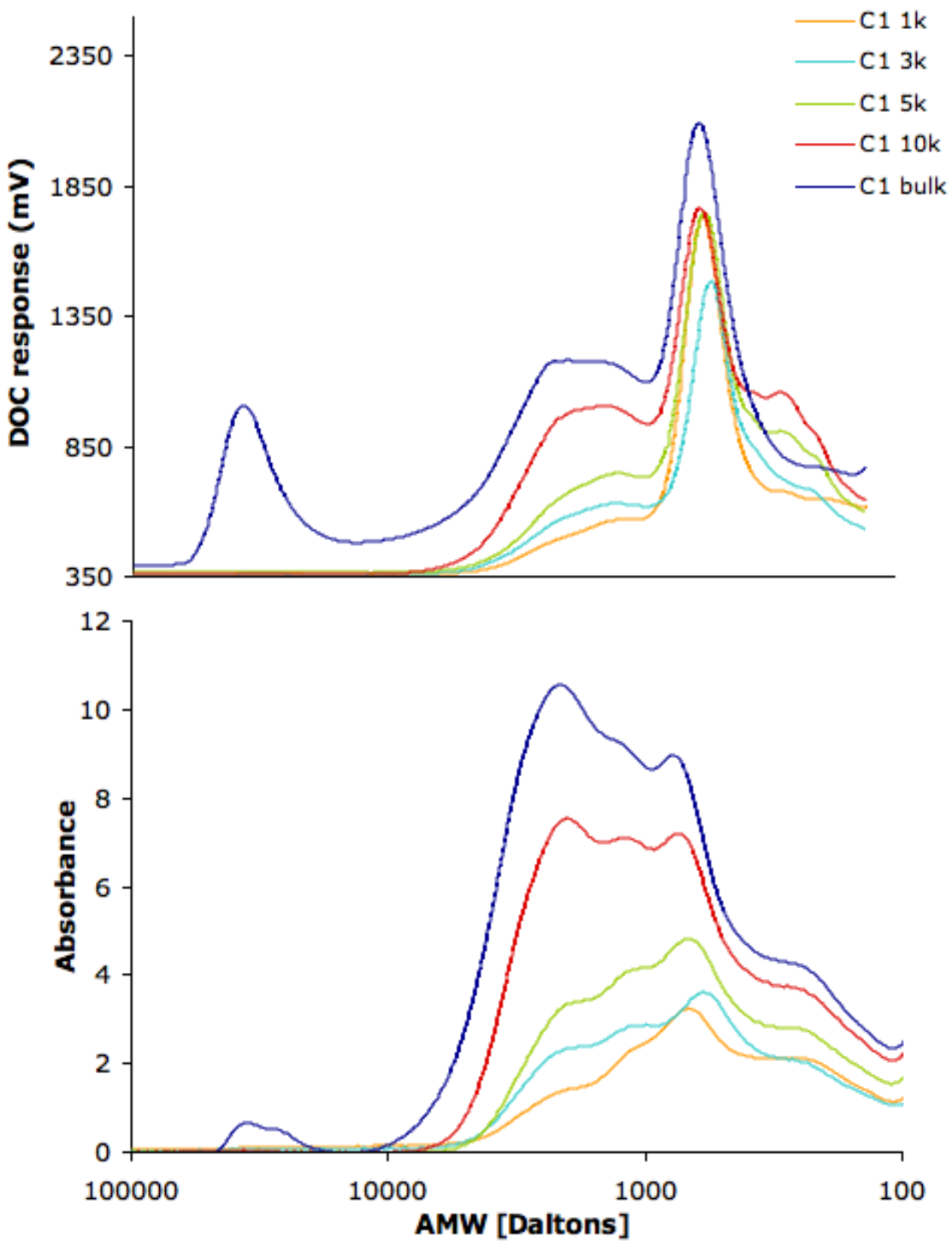

Figure 4.1: Size Exclusion Chromatography for the C1 sample and fractions. Both the DOC and UV response are plotted. Conditions: buffer (0.0024 M NaH_2PO_4, 0.0016 M Na_2HPO_4, and 0.025 M Na_2SO_4 adjusted to pH 6.8 ± 0.1), 1.0 mL/min flow rate, 2.0 µL/min acid and oxidizer flow rate.

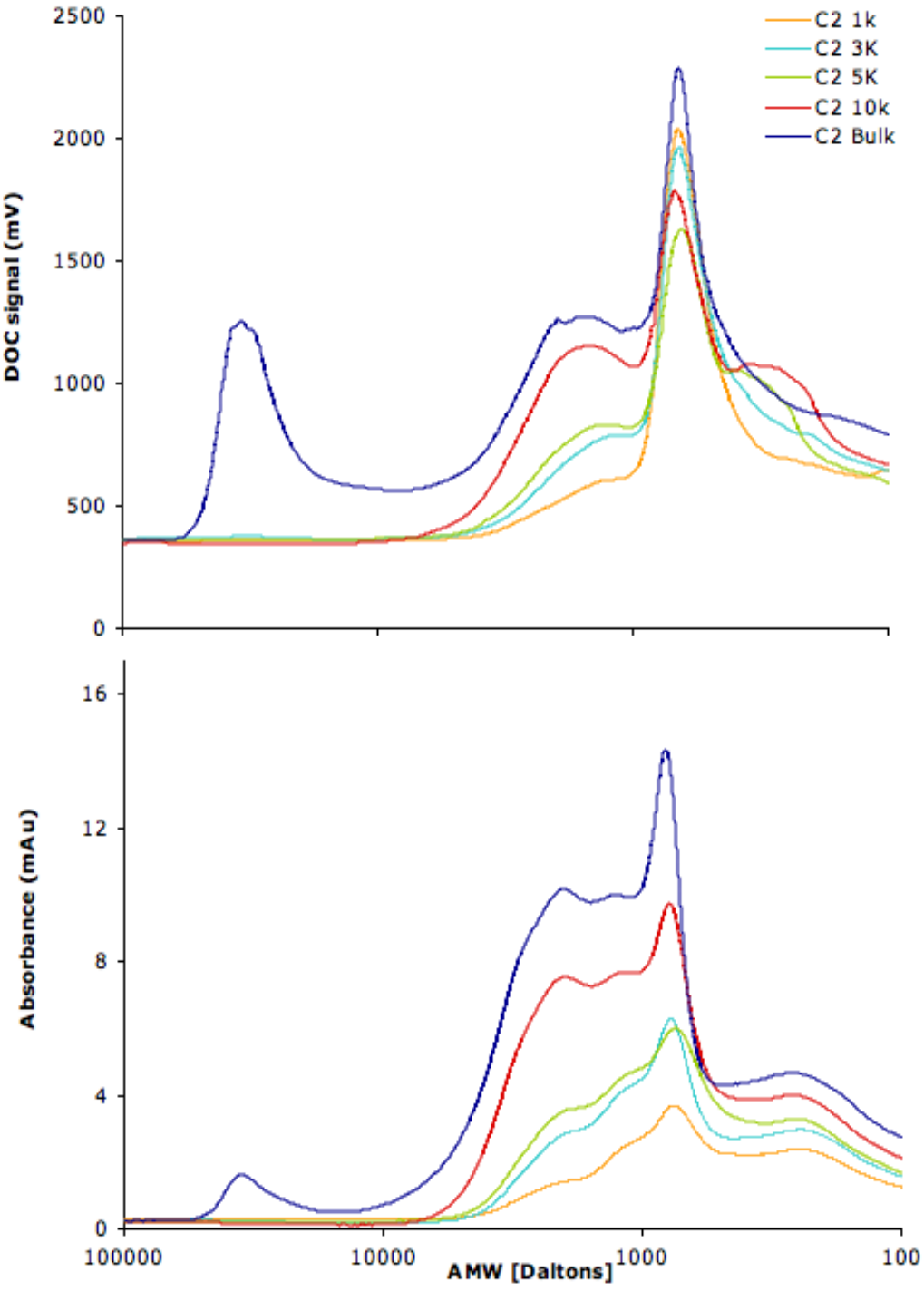

Figure 4.2: Size Exclusion Chromatography for the C2 sample and fractions. Both the DOC and UV response are plotted. Conditions: buffer (0.0024 M NaH_2PO_4, 0.0016 M Na_2HPO_4, and 0.025 M Na_2SO_4 adjusted to pH 6.8 ± 0.1), 1.0 mL/min flow rate, 2.0 µL/min acid and oxidizer flow rate.

4.2: Kinetics of Ozone Decomposition

Figure 4.3 through 4.6 illustrate that the pseudo first order reaction kinetics between ozone and the fractionated wastewater samples. Ozone decay curves were successfully modeled as a first order decay rates ($R^2 > 0.98$) for each of the bulk and fractionated samples.

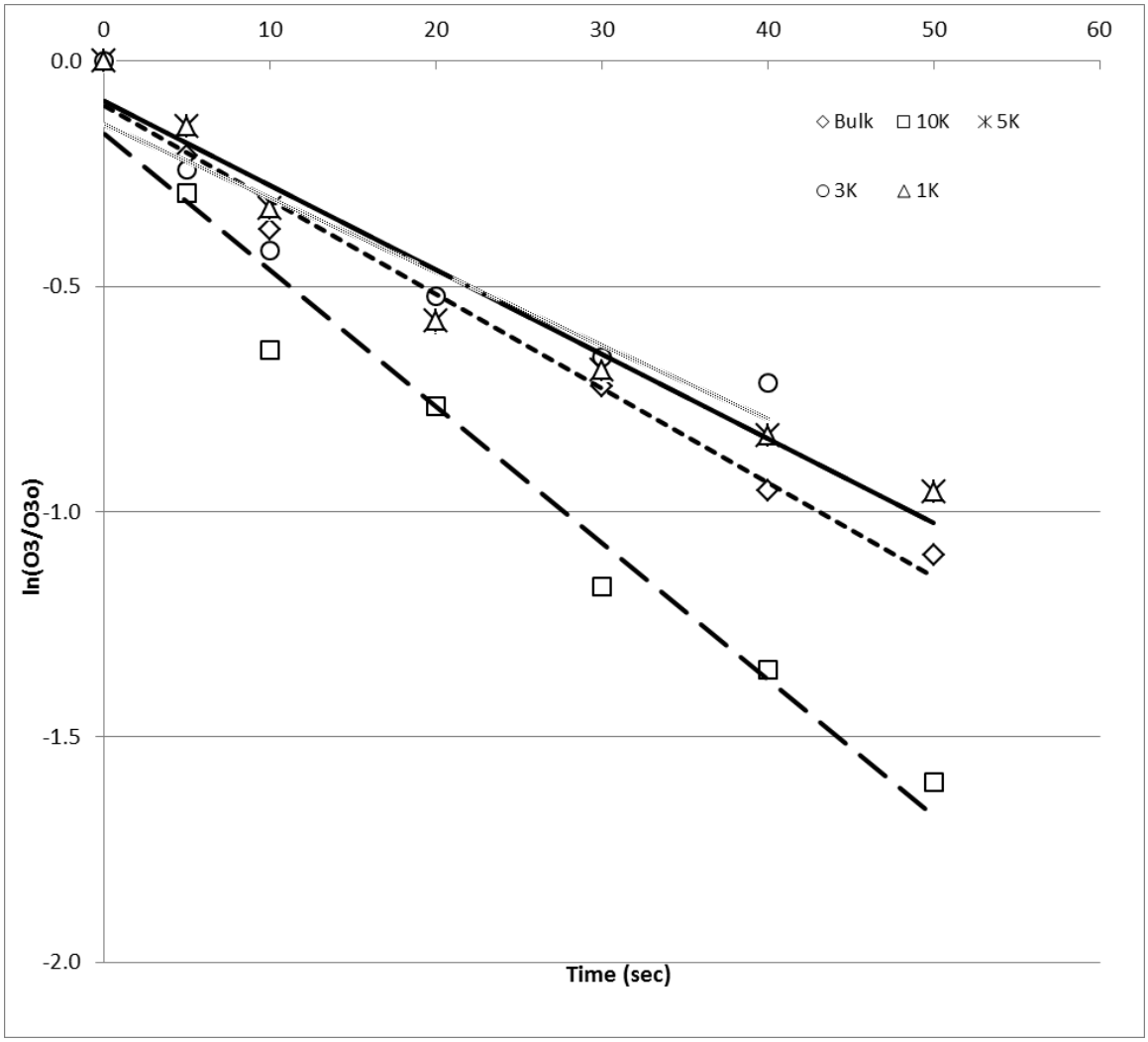

Figure 4.3: Pseudo first order decay rate constants for A sample and fractions. Ozone stock solution (~60 mg/L) was spiked into each fraction on a 1:1 DOC:Ozone ratio. The <10 kDa fraction is shown to be the most reactive.

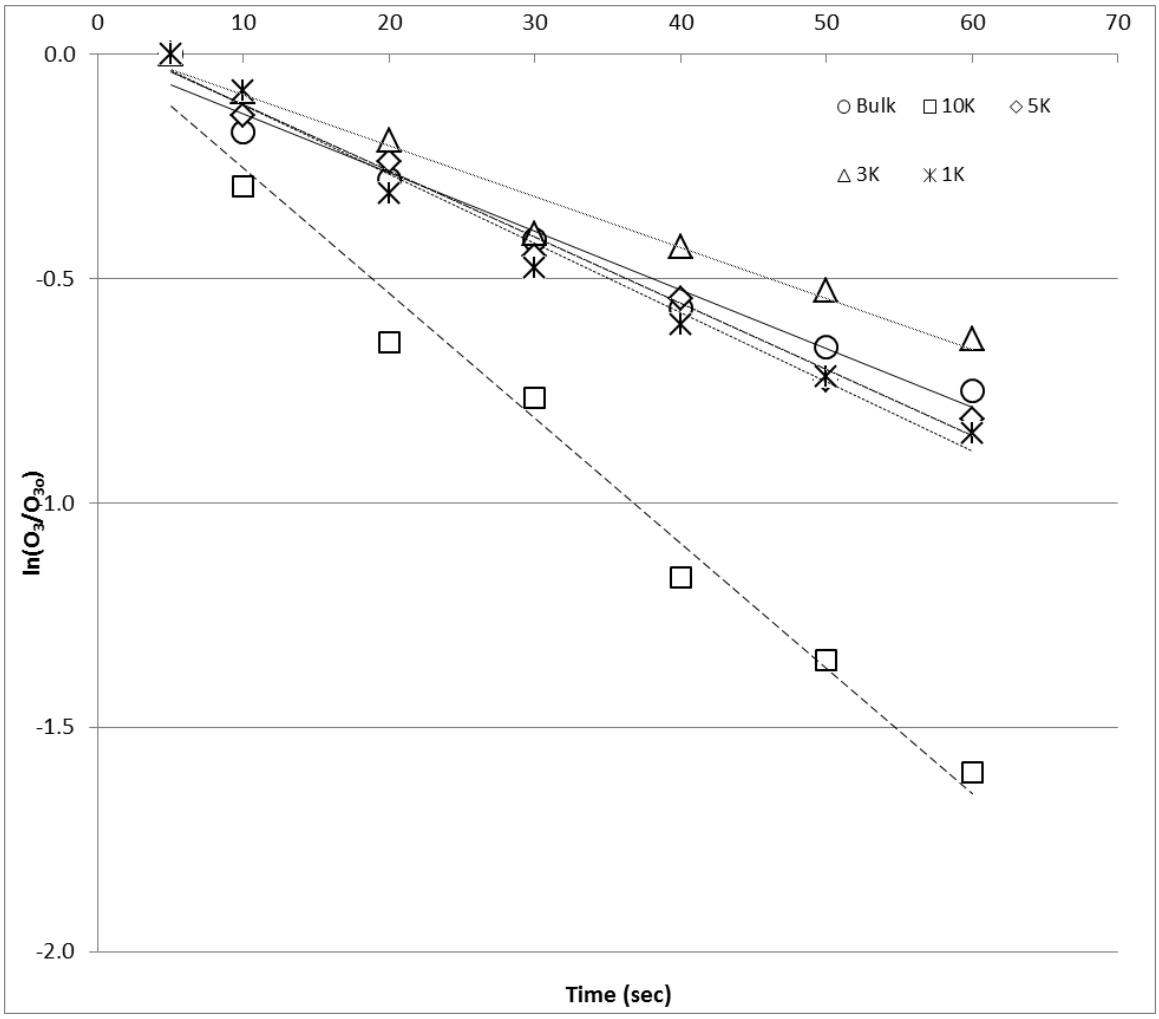

Figure 4.4: Pseudo first order decay rate constants for B sample and fractions. Ozone stock solution (~60 mg/L) was spiked into each fraction on a 1:1 DOC:Ozone ratio. The <10 kDa fraction is shown to be the most reactive.

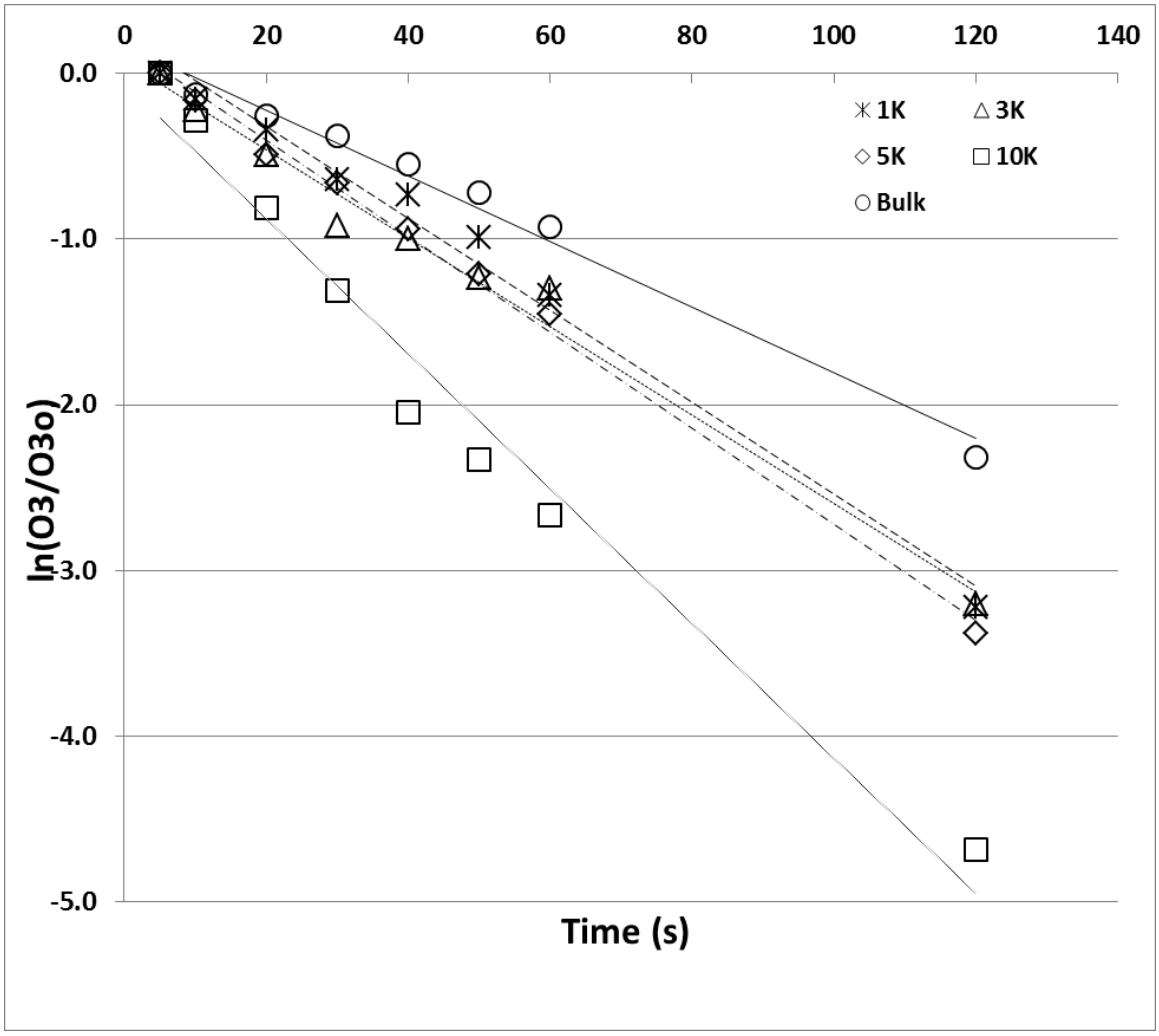

Figure 4.5: Pseudo first order decay rate constants for C1 sample and fractions. Ozone stock solution (~60 mg/L) was spiked into each fraction on a 1:1 DOC:Ozone ratio. The <10 kDa fraction is shown to be the most reactive.

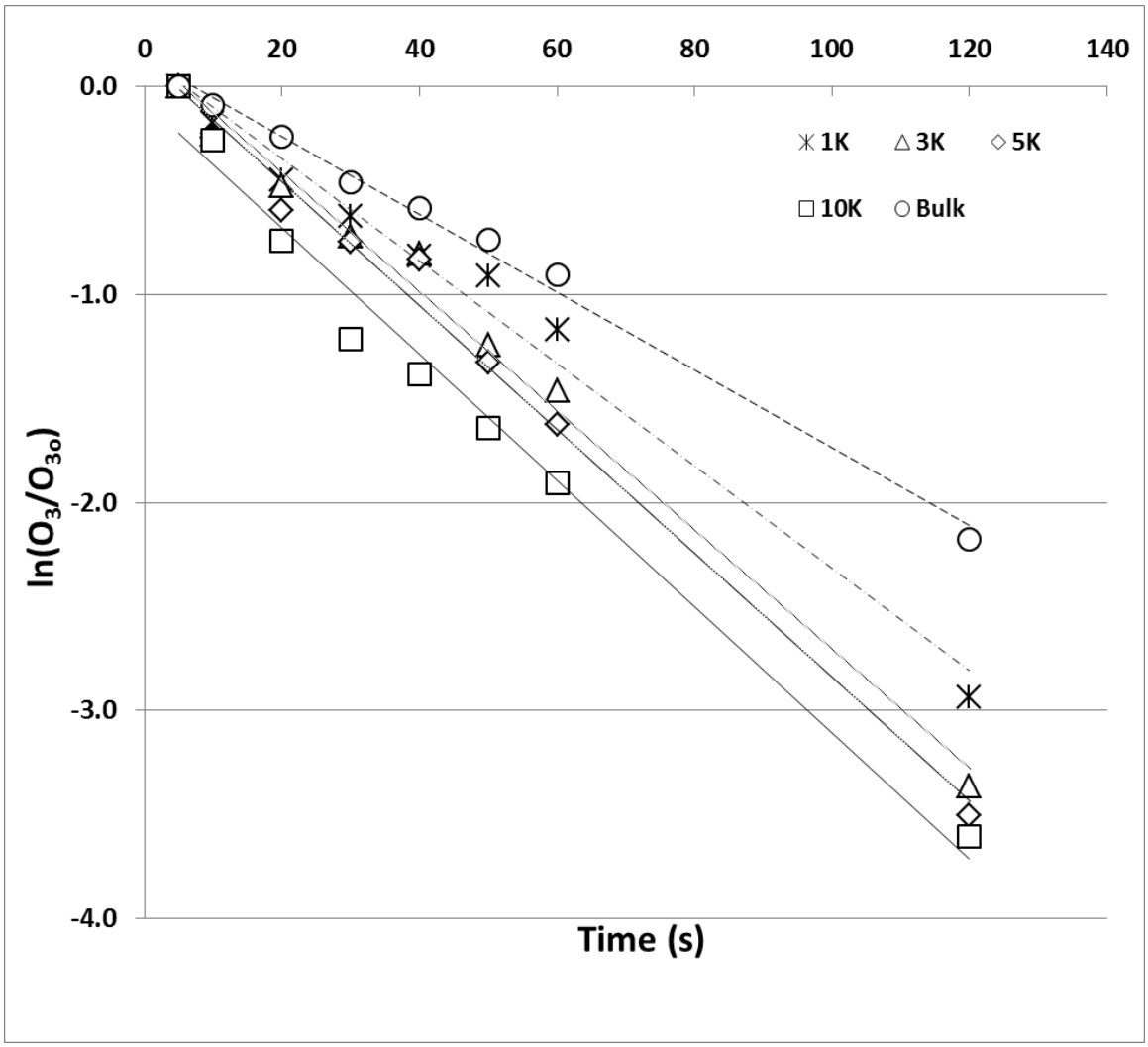

Figure 4.6: Pseudo first order decay rate constants for C2 sample and fractions. Ozone stock solution (~60 mg/L) was spiked into each fraction on a 1:1 DOC:Ozone ratio. The <10 kDa fraction is shown to be the most reactive.

An ozone dose of a 1:1 ozone:DOC ratio was added to each of the samples and fractions. This ozone dose was chosen in order to normalize all ozone reactions to the DOC concentration. The pseudo first-order ozone decay rates (k_{O3}) obtained from the ozone decay are displayed in Table 4.6 through 4.8. The k_{O3} values are shown with confidence intervals of 95%.

Each of the four waters followed the same general trend of a significant increase in k_{O3} from the bulk to the <10k fraction. It is shown that k_{O3} for the <10 kDa fraction is

significantly greater than the other fractions for samples B and C2. Samples A and C1 showed greater values for the $k_{O3\text{-}EfOM}$ in the <10 kDa fraction.

Table 4.5: Ozone Kinetic Characteristics of Fractionated A Water

Fraction (kDa)	k_{O3} (s^{-1})
A	
Bulk	0.0193 ± 0.0023
<10	0.0244 ± 0.0034
<5	0.0173 ± 0.0012
<3	0.0150 ± 0.0106
<1	0.0161 ± 0.0028

Table 4.6: Ozone Kinetic Characteristics of Fractionated B Water

Fraction (kDa)	k_{O3} (s^{-1})
B	
Bulk	0.0131 ± 0.0007
<10	0.0309 ± 0.0126
<5	0.0152 ± 0.0032
<3	0.0114 ± 0.0006
<1	0.0158 ± 0.0027

Table 4.7: Ozone Kinetic Characteristics of Fractionated C1 and C2 Water

Fraction (kDa)	k_{O3} (s^{-1})
C1	
Bulk	0.0164 ± 0.0018
<10	0.0338 ± 0.0064
<5	0.0272 ± 0.0045
<3	0.0254 ± 0.0034
<1	0.0202 ± 0.0025
C2	
Bulk	0.0160 ± 0.0022
<10	0.0504 ± 0.0047
<5	0.0265 ± 0.0045
<3	0.0244 ± 0.0044
<1	0.0233 ± 0.0011

The data illustrated in Table 4.5 through 4.7 suggests that the influence of both the high and low molecular weight compounds result in an overall decrease in k_{O3}. This is consistent with the understanding of ozone reactivity and the characteristics of the >10 kDa and <1 kDa fractions. The low aromatic colloid material in the >10 kDa fraction and the hydrophilic material of the <1 kDa fraction do not contain a high degree of electron donating functional groups that are attacked preferentially by ozone. The more aromatic moieties of the 10 – 1 kDa fraction are expected to have high degree of aromaticity. The significant increase in k_{O3} from the bulk to <10 kDa fraction corresponds the removal of the non reactive large polysaccharide material.

Each of the sample's fractions consists of different varieties and concentrations of EfOM. The bulk fraction contains the entire variety of large molecular weight polysaccharides and cellular debris as well as the humic, fulvic and aromatic organic matter and low molecular weight UAP (Boero 1996). The <10 kDa fraction does not contain the large organic colloid material but consists of the remaining organic mixture. The <5 kDa and <3 kDa fractions contain the more aromatic and fulvic-like organic matter and the <1 kDa fraction consists of the small, hydrophilic UAP (Boero 1996; Her 2003; Allpike, Heitz et al. 2005).

Since the inorganic characteristics of the samples are consistent throughout the fractions, any difference in observed ozone reactivity is due to the differences in EfOM. The k_{O3} rates are different in each fraction throughout the reaction indicating that the EfOM reaction pathway of ozone is significant throughout the ozone decomposition. The difference in ozone decay rates with each of the fractions supports the hypothesis stated by other researhers that the ozone decomposition in wastewaters is dominated by

reactions between ozone and very specific EfOM moieties throughout the reaction (Buffle, Schumacher et al. 2006).

Figures 4.7 and 4.8 illustrate the ozone exposure as a function of time for the C1 and C2 samples and fractions. The ozone exposure is calculated by integrating the area underneath the ozone decay curve for each sample. The two plots show that ozone is present in the bulk water system much longer than any of the fractionated waters.

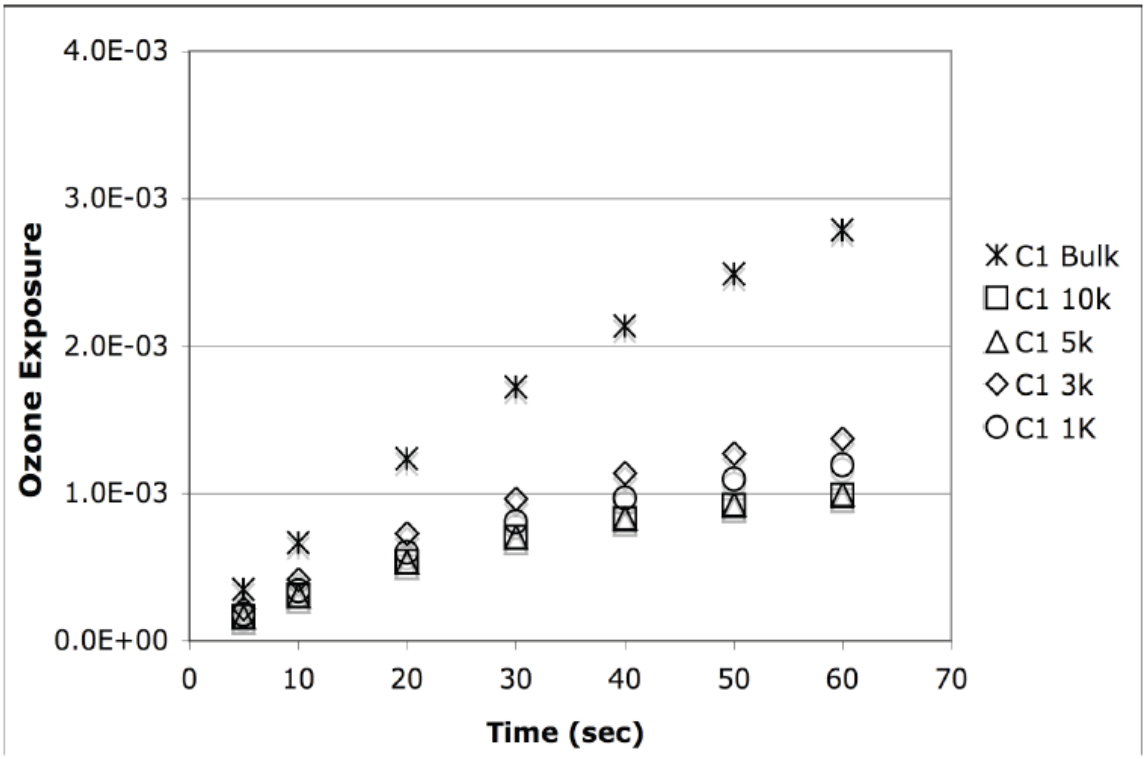

Figure 4.7: The ozone exposure for the C1 fractions. The bulk water has the highest ozone exposure compared to the fractions.

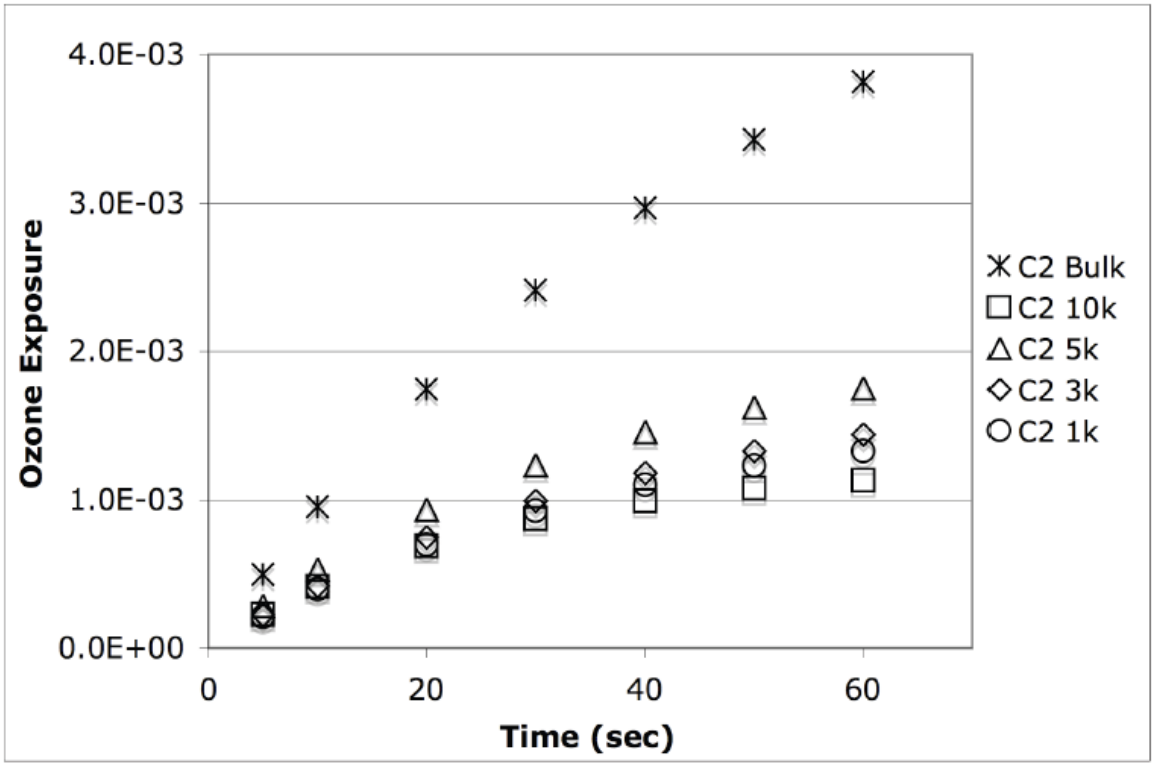

Figure 4.8: The ozone exposure for the C2 fractions. Like the C1 sample, the bulk water has the highest ozone exposure compared to the fractions.

In both C1 and C2 waters the bulk fraction has the highest exposure out of all the fractions. This is due to the relative un-reactive nature of the > 10 kDa fraction of EfOM. This un-reactive nature was previously shown in the pseudo first order ozone decay of both waters. Figures 4.7 and 4.8 also show that the <10 kDa fractions in both the C1 and C2 waters display the lowest ozone exposures. This is also explained by the very reactive nature of the <10 kDa fraction previously shown as the highest pseudo first order decay of both fractions.

4.3: Measurement of R_{CT}

The R_{CT} relationships developed obtained for the fractionated waters are displayed in Table 4.8 through 4.10. The ozone and $HO^{\bullet}$ exposures of each sample were run in triplicate and the values are reported with a confidence interval of 95%.

Table 4.8: R_{CT} values for A Water

Fraction (kDa)	R_{CT} ($x10^{-8}$)
A	
Bulk	4.78 ± 0.13
<10	7.79 ± 0.89
<5	5.29 ± 0.18
<3	6.48 ± 1.36
<1	3.90 ± 0.21

Table 4.9: R_{CT} values for B Water

Fraction (kDa)	R_{CT} ($x10^{-8}$)
B	
Bulk	5.24 ± 0.21
<10	9.39 ± 1.27
<5	6.03 ± 0.29
<3	7.22 ± 0.25
<1	5.41 ± 0.18

Table 4.10: R_{CT} values for C1 and C2 Water

Fraction (kDa)	R_{CT} ($x10^{-8}$)
C1	
Bulk	6.31 ± 0.21
<10	18.6 ± 2.75
<5	11.3 ± 1.25
<3	10.2 ± 0.47
<1	5.94 ± 2.96
C2	
Bulk	5.55 ± 0.15
<10	15.4 ± 0.88
<5	8.28 ± 0.86
<3	6.56 ± 0.83
<1	7.24 ± 0.43

The R_{CT} relationships in all the samples demonstrate a significant increase from the bulk to the <10 kDa fraction and then a steady decrease in R_{CT} from the <10 to the <1 kDa fractions. An increase in R_{CT} signifies an increased $HO^{\bullet}$ exposure for a given ozone exposure. The increase in R_{CT} from the bulk to the <10 kDa fraction is attributed to the removal of the large molecular weight organic colloids and polysaccharides. Ozone has a low reactivity for aliphatic chains in polysaccharides particularly from the C-H bonds (Mvula 2009).

Figure 4.9 illustrates the R_{CT} for the A and B samples. The two waters demonstrate the same trend where the <10 kDa fraction is the largest followed by the < 3 kDa fraction. These differences in these values are not as pronounced as the C1 and C2 waters.

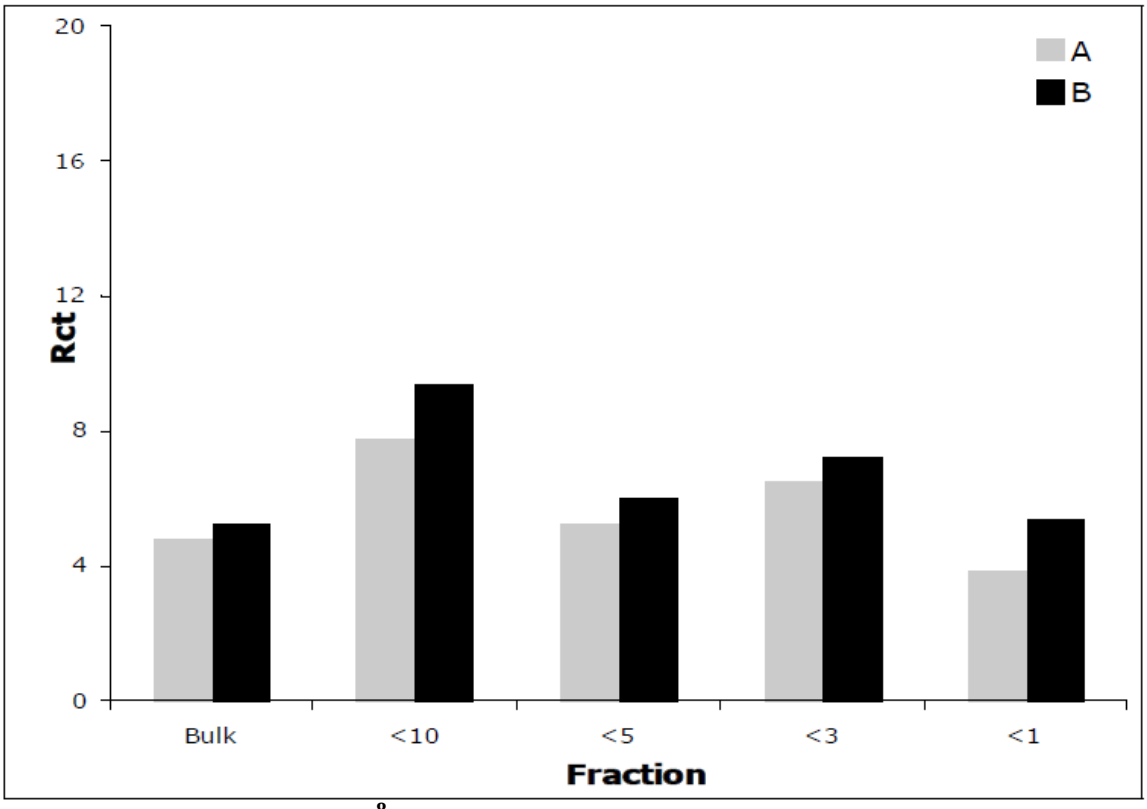

Figure 4.9: R_{CT} values ($x10^{-8}$) of both A and B fractions. The < 10 kDa fraction displays the highest reactivity.

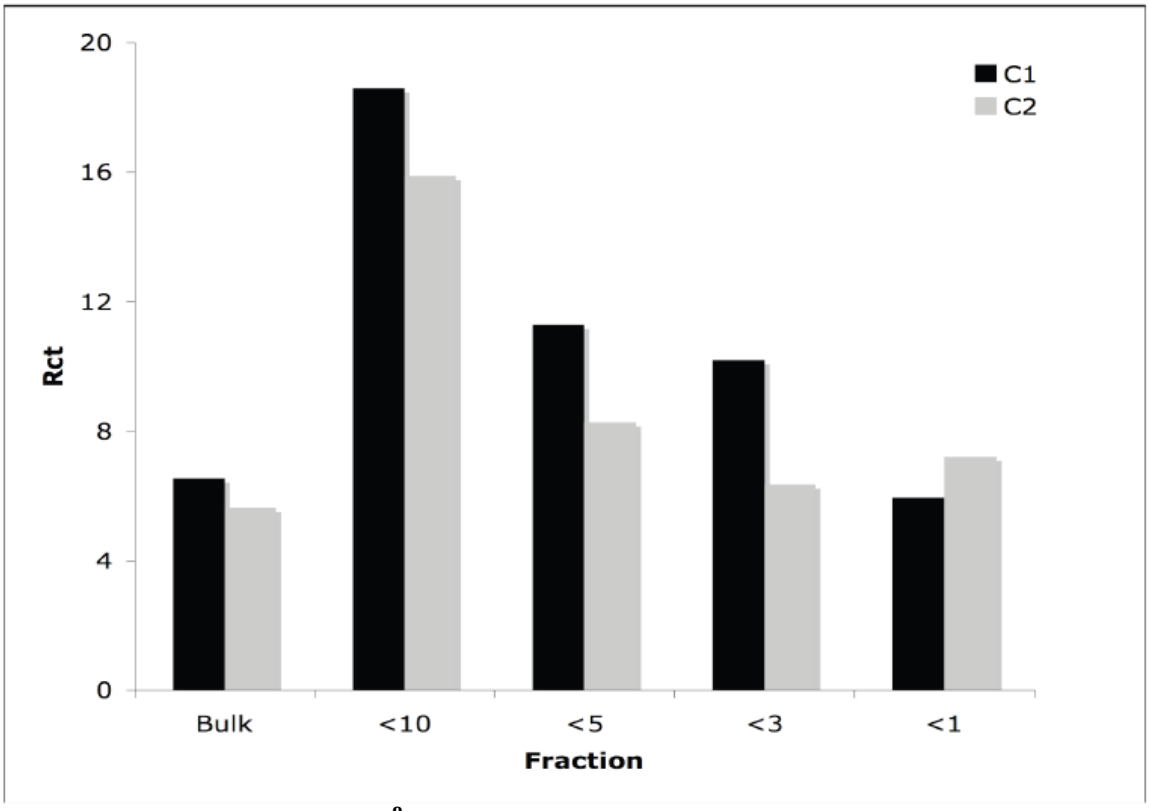

Figure 4.10: R_{CT} values (x10^{-8}) of both C1 and C2 samples and fractions. The < 10 kDa fraction has the highest R_{CT} which steadily decreases as the AMW fractions decrease.

Figure 4.10 demonstrates a much more pronounced increase in R_{CT} from the bulk to the < 10k fractions. This large increase was observed on all the samples as well as a steady decrease in R_{CT} from the <10k to the <1k fractions. The steady decrease in R_{CT} from the < 10 kDa to the < 1 kDa fraction indicates that the EfOM between 10 and 1 kDa fraction are the most reactive and the > 10 kDa and < 1 kDa fractions produce the least amount of $HO^{\bullet}$ per unit of ozone.

Table 4.11: Difference in DOC and Ozone Kinetics from Bulk to <10 kDa Fractions

Sample (Davis, Talukdar et al.)	A	B	C1	C2
ΔDOC (mg/L)	1.4	0.9	1.9	3.7
Δ k_{O3}	0.0051	0.0178	0.0174	0.0344
Δ R_{CT}	3.01	4.15	12.29	9.85

Table 4.11 shows the EfOM contained in the >10 kDa fraction as well as the increase in k_{O3} and R_{CT}. There is no relationship between the amount of organic matter >10 kDa fraction and increase in reactivity suggesting that the properties of EfOM rather than the concentration is the most important parameter. Wastewater treatment greatly impacts the composition of the >10 kDa fraction. An example of this is aerated lagoon type systems and poor advanced biological treatment systems (nitrification/denitrification) show the same >10 kDa signatures which differ from both membrane batch reactors (MBR) and trickling filters (Song 2010). The treatment process in A and C1 samples both employ partial nitrification/denitrification treatment. The B samples have complete nitrification/denitrification and the C2 sample does not have any advanced treatment.

4.4 Formation rate of $HO^{\bullet}$ from EfOM

From the results presented above, it is clear that not all fractions of EfOM behave the same during the decomposition of ozone. It has been shown that high and low molecular weight fractions (>10 kDa and <5kDa) result in lower ozone decay and yield of $HO^{\bullet}$.

The overall formation of $HO^{\bullet}$ is a function of both formation and decay rates. These two contributions could be expressed mathematically by expression 4.1

$$\frac{d[HO^{\bullet}]}{dt} = F - [HO^{\bullet}]\left(k_p[P] + \sum k_{si}[S_i]\right) \qquad (4.1)$$

where F is the formation of $HO^{\bullet}$ from both the water and organic matter pathway and the second term is the overall scavenging.

$$F = K_x[DOM] + K_y[OH^-] \quad (4.2)$$

k_p is the reaction rate constant of $HO^{\bullet}$ with the probe compound, [P] is the concentration of the probe compound, k_{si} is the reaction rate constant of $HO^{\bullet}$ with the scavenging species and $[S_i]$ is the concentration of the scavenging species.

The scavenging components taken into account when modeling the formation of $HO^{\bullet}$ were the inorganic constituents (ammonia, nitrate/nitrite and alkalinity) and the EfOM. Reaction rate constants between $HO^{\bullet}$ and the inorganic constituents are established in the literature (Buxton, Greenstock et al. 1988; Hickel 1992; Logager 1993). The reaction rate constant between $HO^{\bullet}$ and each EfOM ($k_{HO\text{-}EfOM}$) fraction were obtained for the C1 and C2 waters using pulse radiolysis described in detail previously (Whitham, Lyons et al. 1995). Table 4.12 summarizes $k_{HO\text{-}EfOM}$ for the C1 and C2 fractions. The general trend shown in the C1 and C2 samples is an increase in $k_{HO\text{-}EfOM}$ as the AMW fraction decreases.

Table 4.12: Reaction Rate Constants between $HO^{\bullet}$ and C1 and C2 Fractions

Fraction (kDa)	$k_{HO\text{-}EfOM}$ ($M^{-1}s^{-1}$)
C1	
Bulk	1.03×10^{9}
<10	1.24×10^{9}
<5	1.30×10^{9}
<3	2.59×10^{9}
<1	1.38×10^{9}
C2	
Bulk	7.18×10^{8}
<10	1.16×10^{9}
<5	1.47×10^{9}
<3	1.76×10^{9}
<1	3.99×10^{9}

The probe used to indirectly measure $HO^{\bullet}$ was para-chlorobenzoic acid (pCBA). The relationship between $HO^{\bullet}$ exposure and the oxidation of pCBA is:

$$\int [HO^{\bullet}]dt = \frac{\ln\left(\frac{[pCBA]}{[pCBA]_o}\right)}{-k_{HO^{\bullet}\,pCBA}} \tag{4.3}$$

The $HO^{\bullet}$ concentration was calculated by taking the derivative of the $HO^{\bullet}$ exposure gives the $HO^{\bullet}$ concentration as a function of time:

$$[HO^{\bullet}] = d\frac{\left(\int [HO^{\bullet}]dt\right)}{dt} \tag{4.4}$$

From these relationships it is possible to back-calculate the overall decay of $HO^{\bullet}$.

Table 4.13 and 4.14 summarize the formation rate of $HO^{\bullet}$, $HO^{\bullet}$ exposure and ozone exposure at a time of 30 seconds for the C1 and C2 waters respectively.

For the C1 and C2 waters respectively, >97% and >82% of the $HO^{\bullet}$ production comes from the <10 kDa fraction. This supports the idea that the >10 kDa fraction of organic matter do not contribute to the EfOM- $HO^{\bullet}$ formation pathway.

Table 4.13: The $HO^{\bullet}$ Formation Rate, $HO^{\bullet}$ Exposures and Ozone Exposures for Site C1

Fraction (kDa)	At t = 30 seconds		
	$HO^{\bullet}$ Formation	$HO^{\bullet}$ Exposure	Ozone Exposure
Bulk	4.89×10^{-6}	2.62×10^{-10}	1.72×10^{-3}
<10	4.75×10^{-6}	2.89×10^{-10}	7.03×10^{-4}
<5	2.58×10^{-6}	2.01×10^{-10}	7.08×10^{-4}
<3	4.01×10^{-6}	2.11×10^{-10}	9.63×10^{-4}
<1	1.82×10^{-6}	1.46×10^{-10}	8.08×10^{-4}

The C1 water shows the < 3 kDa has a $HO^{\bullet}$ formation greater than the < 5 kDa fraction. This is a result of the model used to calculate the $HO^{\bullet}$ formation rate. The formation is calculated as the sum of the scavenging due to organic and inorganic constituents. The < 3 kDa fraction has a significantly higher $k_{HO\text{-}EfOM}$ compared to the < 5 kDa fraction giving it a higher formation.

Table 4.14: The $HO^{\bullet}$ Formation Rate, $HO^{\bullet}$ Exposures and Ozone Exposures for Site C2

Fraction (kDa)	At t = 30 seconds		
	$HO^{\bullet}$ Formation	$HO^{\bullet}$ Exposure	Ozone Exposure
Bulk	7.11×10^{-6}	2.96×10^{-10}	2.41×10^{-3}
<10	5.87×10^{-6}	2.72×10^{-10}	8.73×10^{-4}
<5	4.73×10^{-6}	2.04×10^{-10}	1.23×10^{-3}
<3	3.10×10^{-6}	1.58×10^{-10}	9.93×10^{-4}
<1	3.79×10^{-6}	1.46×10^{-10}	9.27×10^{-4}

The formation of $HO^{\bullet}$ is not at steady state throughout the reaction. The initial $HO^{\bullet}$ formation is high due to the rapid reacting organic species with the higher ozone concentrations that create large amounts of $HO^{\bullet}$. As the concentration of ozone decreases the formation rate of $HO^{\bullet}$ decreases.

Figure 4.11 and 4.12 illustrate the $HO^{\bullet}$ exposure over time for both the C1 and C2 fractions. The bulk and <10 kDa fraction in the C1 water have similar $HO^{\bullet}$ exposures as do the <3 kDa and <5 kDa fractions.

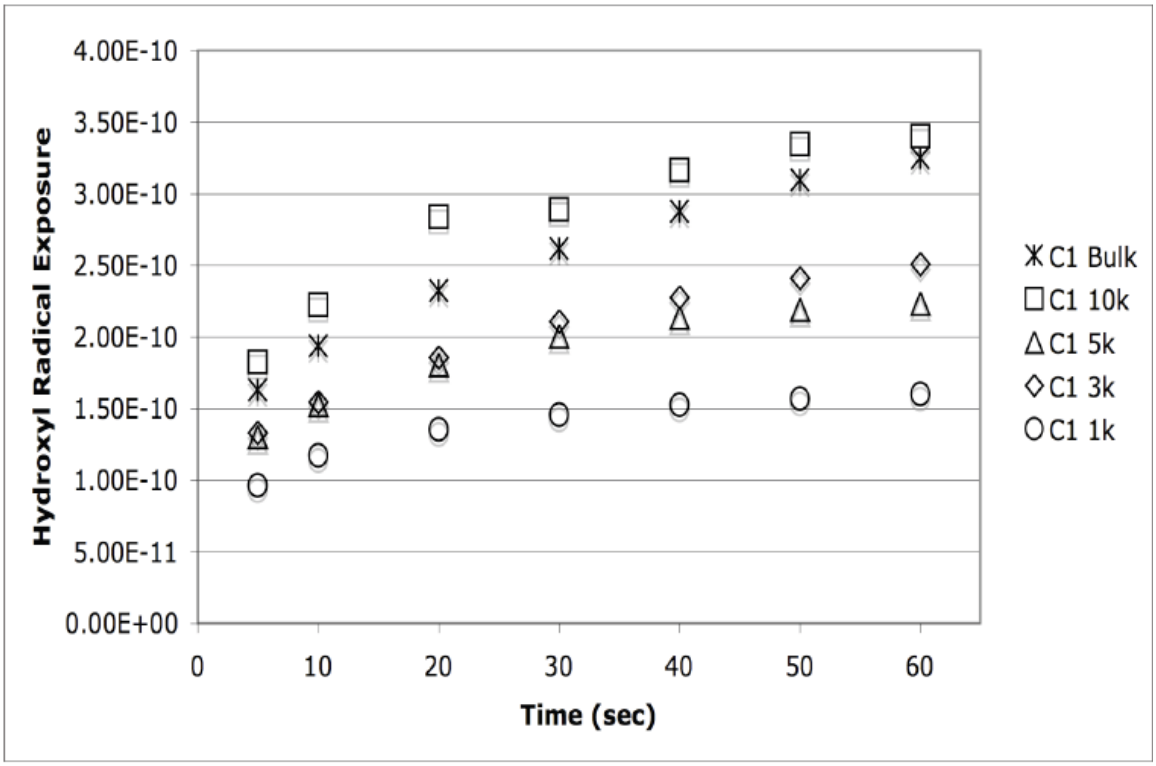

Figure 4.11 The $HO^{\bullet}$ exposure as a function of time for the C1 fractions. The <10 kDa fraction had the highest exposure followed by the bulk

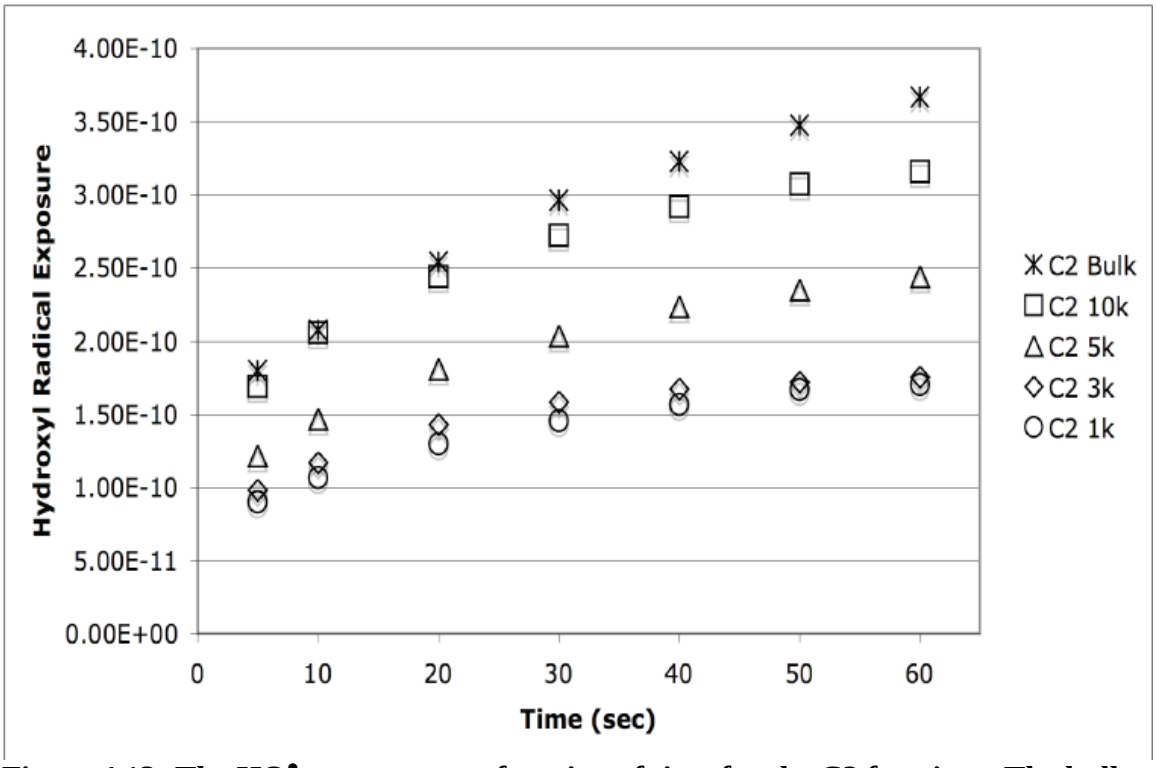

Figure 4.12: The HO• exposure as a function of time for the C2 fractions. The bulk fraction had the highest formation followed by the <10 kDa fraction

The HO• exposures for the C2 fractions did not display the same trend as the C1 fractions. For the C2 water the bulk and < 10 kDa started out with the same HO• exposure but the exposure in the < 10 kDa levels off when the ozone in the system has completely reacted. Because the organic matter present in the < 10 kDa fraction is more reactive than the > 10 kDa, the ozone remains in the system longer and continues to form HO•. The < 3 kDa and < 1 kDa waters have very similar HO• exposures throughout the reactions. This data confirms that the > 10 kDa and < 1 kDa fractions do not contribute to the formation of HO• compared to the formation contribution of the fraction between 10 and 5 kDa.

4.5: Use of Coagulation to Enhance Ozone Efficiency

Preliminary jar tests were run on the C2 water to determine if the large weight polysaccharides and cellular debris could be removed through a simple coagulation step. Iron chloride ($FeCl_3$) was chosen as the coagulant because of its current use in wastewater facilities. Three different coagulant doses, 5.5, 11, and 16 mg/L, were chosen. The water that was dosed with 16 mg/L of $FeCl_3$ was then taken and compared to the original bulk water. Table 4.15 shows the general water quality characteristics of the bulk and coagulated water.

Table 4.15: Water Quality for the C2 Bulk and Coagulated Water

Sample	DOC (mg/L)	UV_{254}	SUVA
C2	11.7	0.17	1.43
C2 Coagulation	10.1	0.15	1.49

The reduction in the DOC shows that there was organic matter removal through coagulation. The UV_{254} values decreased due to the removal of organic matter from the water.

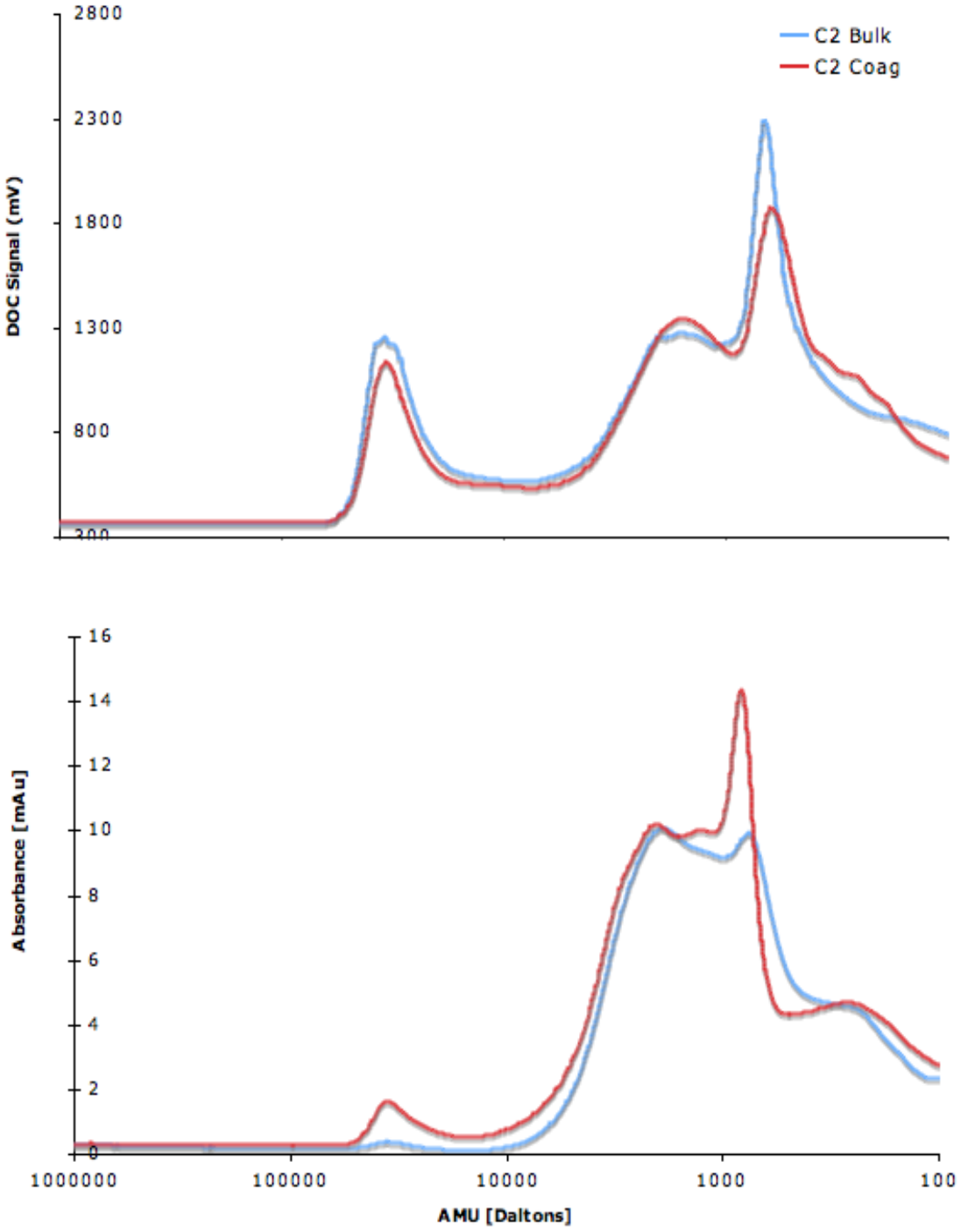

Figure 4.13: Size Exclusion Chromatography on the bulk and coagulated C2 sample. Both the DOC and UV response are plotted. Conditions: buffer (0.0024 M NaH_2PO_4, 0.0016 M Na_2HPO_4, and 0.025 M Na_2SO_4 adjusted to pH 6.8 ± 0.1), 1.0 mL/min flow rate, 2.0 μL/min acid and oxidizer flow rate

Figure 4.13 shows the SEC DOC and UV response plot for the C2 bulk and coagulated sample. The DOC response shows that as predicted there was a decrease in the first peak, (~30 kDa) from the bulk to the coagulated water.

To determine if the partial removal of the large molecular weight organic matter would have an effect on the reactions of ozone as an AOP process, the R_{CT} and k_{O3} rate constant was determined using the same 1:1 TOC:Ozone dose as the bulk water.

Table 4.16: Kinetic Characteristics of Bulk and Coagulated C2 Waters

Sample	k_{O3} (sec^{-1})	R_{CT} (10^{-8})
Bulk	0.0174	5.65
Coagulated	0.0320	8.79

The kinetic data shown in Table 4.16 shows that there is an increase in both the k_{O3} and the R_{CT}. This indicates that using coagulation to target and remove the > 10 kDa fraction will increase the system reactivity.

CHAPTER 5. INFLUENCE OF EfOM ON THE REMOVAL OF MICRO POLLUTANTS

Contaminant testing was preformed on the C2 fractions as well as the coagulated water in order to test the two hypotheses. The first hypothesis is that that the fraction of EfOM between 10 and 5 kDa display the highest ozone reactivity and would correspond to higher micropollutant degradation. The second hypothesis is that the removal of the > 10 kDa fraction by coagulation would also result in an increase in micropollutant degradation.

5.1: Contaminant Removal

Contaminant analysis was run on the C2 bulk sample before ozonation and also on the post ozonated sample and sample fractions (Trenholm, Vanderford et al. 2008). A summary of the initial contaminant concentration as well as the fractions and the coagulated water is given in Table 5.1.

Table 5.1: Contaminant Data for Pre and Post Ozonated C2 Samples

Sample	Pre Ozone	<1k	<3k	<5k	<10k	Bulk	Coag
Atenolol	1900	340	<25	<25	230	520	<25
Carbamazepine	250	<10	<10	<10	<10	<10	<10
Meprobamate	190	140	110	93	140	150	53
Primidone	87	63	30	27	56	62	11
Sulfamethoxazole	530	120	46	28	140	160	<25
TCEP	510	480	350	430	390	450	370
Trimethoprim	460	<10	<10	<10	<10	<10	<10

The contaminants that were selected for testing have a wide range of reactivity with ozone. Carbamazepine, Sulfamethoxazole and Trimethoprim are highly reactive with ozone ($k_{O3} > 10^5$ $M^{-1}s^{-1}$), Atenolol is moderately reactive with ozone ($k_{O3} > 10^3$ $M^{-1}s^{-1}$)

and Meprobamate and TCEP are very uncreative towards ozone ($k_{O3} > 1\ M^{-1}s^{-1}$) (Huber, Canonica et al. 2003). Relative contaminant removal was modeled with the R_{CT} as well as the ozone and $HO^{\bullet}$ exposures. The equation used to model the contaminant removal with the R_{CT} is:

$$\frac{[P]}{[P]_o} = \exp\left\{-\int [O_3]dt\left(k_{HO}R_{CT} + k_{O_3}\right)\right\} \tag{5.1}$$

The equation used to model the contaminant removal with the ozone and $HO^{\bullet}$ exposures is:

$$\frac{[P]}{[P]_o} = \exp\left(-k_{O_3}\int [O_3]dt - k_{HO}\int [^{\bullet}HO]dt\right) \tag{5.2}$$

Figures 5.1. through 5.6 show the observed contaminant removal as well as the predicted contaminant removal using both models for each contaminant.

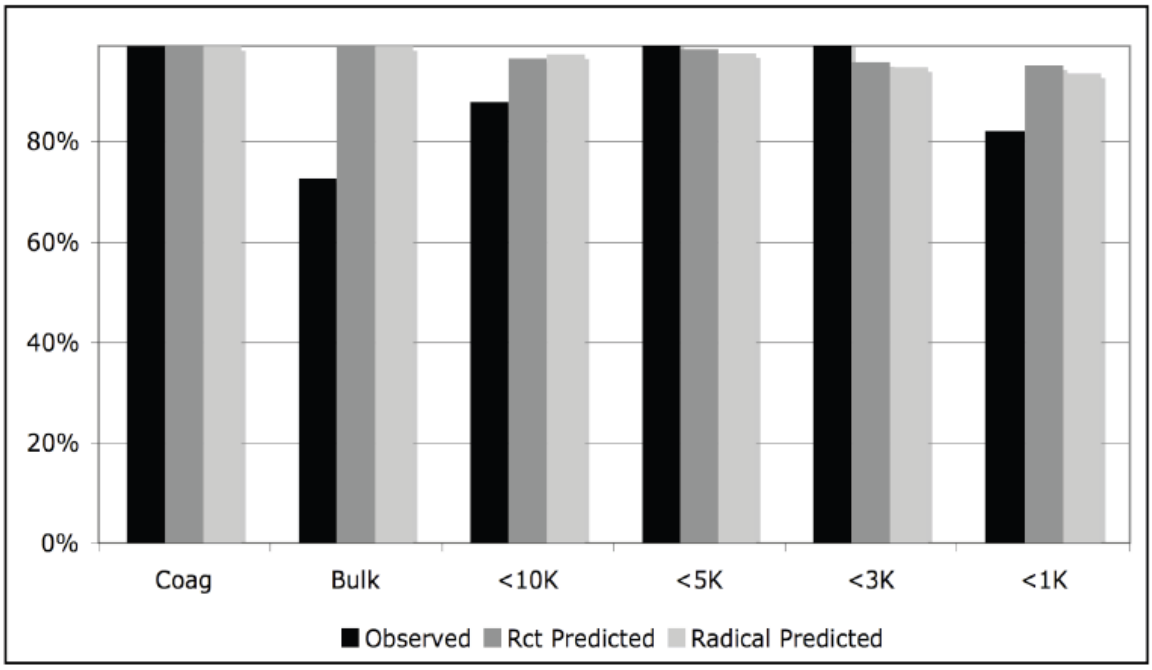

Figure 5.1: Atenolol Removal of C2 Waters and Predicted Removals with R_{CT} and Ozone and $HO^{\bullet}$ Exposures.

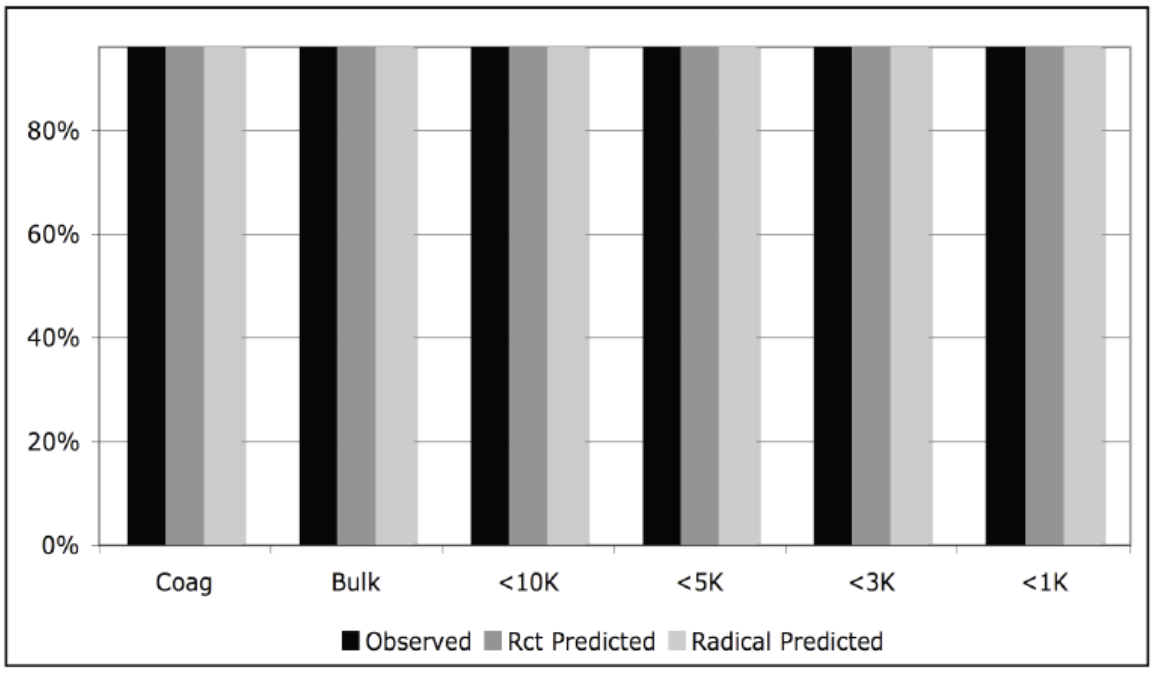

Figure 5.2: Carbamazepine Removal of C2 Waters and Predicted Removals with R_{CT} and Ozone and $HO^{\bullet}$ Exposures.

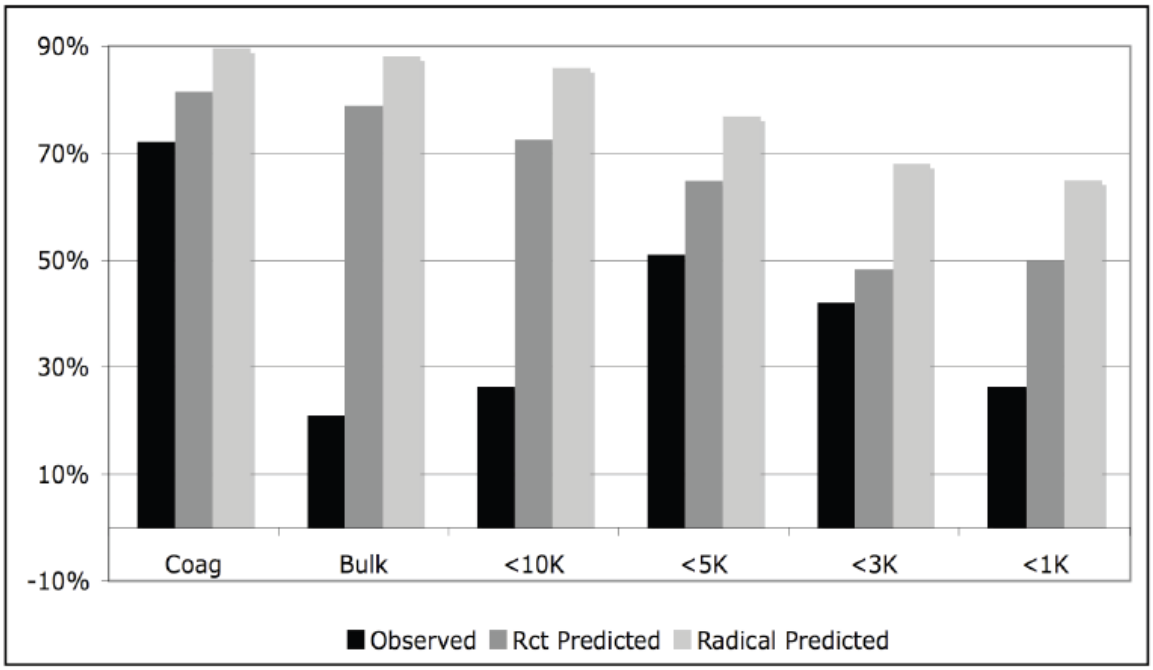

Figure 5.3: Mepobramate Removal of C2 Waters and Predicted Removals with R_{CT} and Ozone and $HO^{\bullet}$ Exposures.

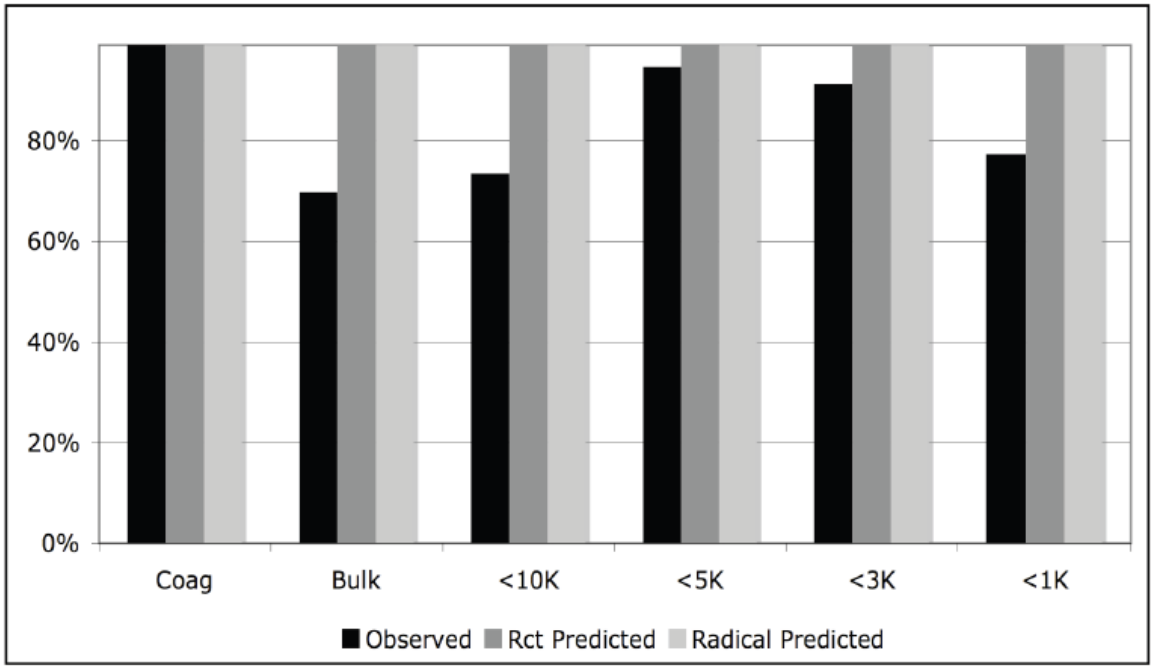

Figure 5.4: Sulfamethoxazole Removal of C2 Waters and Predicted Removals with R_{CT} and Ozone and $HO^{\bullet}$ Exposures.

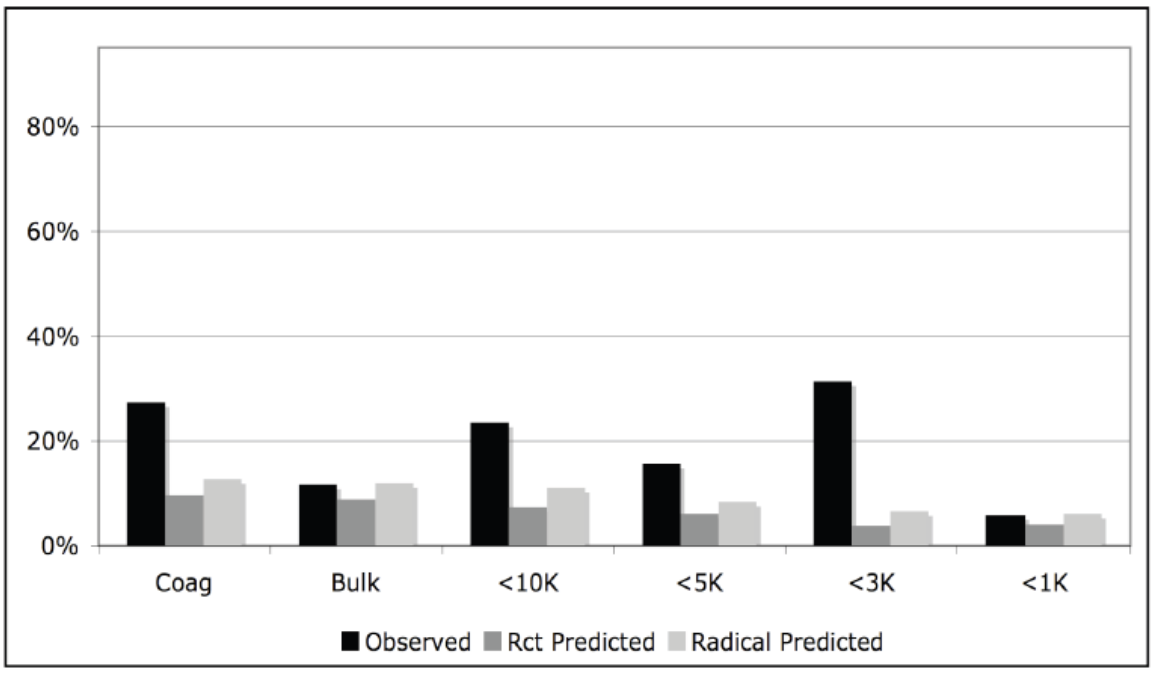

Figure 5.5: TCEP Removal of C2 Waters and Predicted Removals with R_{CT} and Ozone and $HO^{\bullet}$ Exposures.

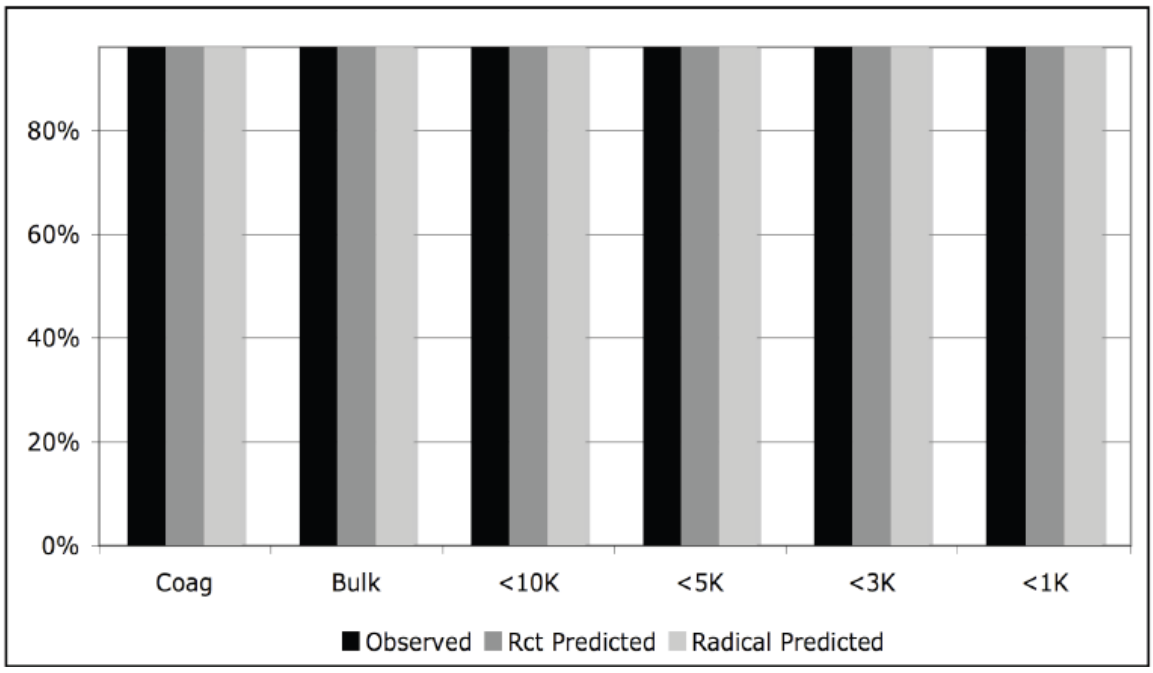

Figure 5.6: Trimethoprim Removal of C2 Waters and Predicted Removals with R_{CT} and Ozone and $HO^{\bullet}$ Exposures.

For the contaminants with a high reactivity with ozone (Atenolol, Carbamazepine and Trimethoprim), the observed relative contaminant removal and the removal predicted by equations 5.1 and 5.2 were in very good agreement. The compounds with low ozone reactivity and varying $HO^{\bullet}$ reactivity had deviations in predicted and measured degree of oxidation. In the case of Meprobamate there is limited contribution of ozone to contaminant oxidation, but the reaction rate constant with $HO^{\bullet}$ is very high (k_{HO}= $7.2x10^{9}$ $M^{-1}s^{-1}$). Both methods of prediction overestimated the oxidation of Meprobamate by as much as 58% with the R_{CT} and 67% with the $HO^{\bullet}$ exposure. Both of the large overestimations are of the < 10 kDa fraction. For TCEP there is also limited contribution of ozone to contaminant oxidation, but the reaction rate with $HO^{\bullet}$ is an order of magnitude less than Meprobamate (k_{HO}= $4.3x10^{8}$ $M^{-1}s^{-1}$). In the case of TCEP, both methods underestimated the contaminant oxidation by up to 27% with the R_{CT} and 20% with the $HO^{\bullet}$ exposure. Both of the large underestimations are of the < 3 kDa fraction.

Previous studies into the oxidation of contaminants and prediction of contaminant removal through ozone and $HO^{\bullet}$ exposure also reported overestimation of $HO^{\bullet}$ selective contaminant oxidation by up to 44% of iopromide (Hollender 2009). Iopromide has very similar reaction kinetics to Meprobamabe in the sense that it has very low ozone reactivity (k_{O3} = 0.5 $M^{-1}s^{-1}$) and very high reactivity with $HO^{\bullet}$ (k_{HO} = $3.1x10^{9}$ $M^{-1}s^{-1}$). The possible explanations for the overestimation given by Hollender et al. is that there is possible short-circuiting in their reactor such that ~15% of the water does not come into contact with ozone and therefore $HO^{\bullet}$. This study was done in a pilot scale plant where gaseous ozone was bubbled into the system.

For the contaminant analysis conducted on the C2 waters a concentrated ozone stock solution (>60 mg_{O3}/L) was spiked into the sample, which was thoroughly mixed, and 100% transfer of ozone dose is assumed. Also, not only did the modeling methods used over predict the contaminant oxidation of Meprobamate but it under estimated the contaminant oxidation of TCEP as well. One possible explanation into the overestimation of contaminant oxidation is the issue of reaction efficiency. It is possible that a specific contaminant, such as Meprobamate, reacts with multiple $HO^{\bullet}$ in a given reaction. However, this phenomenon would be accounted for in the overall $HO^{\bullet}$ reaction rate with that specific compound.

CHAPTER 6. CONCLUSIONS AND FUTURE WORK

6.1: Conclusion

The studies discussed in this thesis looked at the reactions of four fractionated wastewaters (A, B, C1 and C2) and how those different waters reacted with ozone to form $HO^{\bullet}$ for the purpose of contaminant removal. Emphasis was placed on gaining a better understanding of how EfOM of different molecular weights and composition affect the ozone process. In order to gain this better understanding of the influence of EfOM the four wastewaters were fractionated into four different molecular weight cutoffs (< 10 kDa, < 5 kDa, < 3 kDa and < 1 kDa). Each bulk water and fractions were ozonated and various characteristics of the ozone reactions were studied. These characteristics included ozone decay, the R_{CT}, the $HO^{\bullet}$-formation, radical exposure, the effect of coagulation on the bulk sample and micropollutant oxidation and predicted removal.

SEC was preformed on the C1 and C2 samples and the AMW distribution was characterized for the bulk and fractions. The > 10 kDa fraction is characterized as organic colloids that contain polysaccharides. The < 1 kDa fraction are characterized as the small hydrophilic and aliphatic compounds. The fraction between 10 and 1 kDa are characterized as the fulvic-acid material.

The pseudo first order decay of ozone was calculated for the four wastewaters and fractions. The < 10 kDa fraction was found to have a significantly larger k_{O3} rates for sample B and C2. Sample A and C1 also displayed larger k_{O3} rates for the < 10 kDa compared to the other fractions.

The R_{CT} was determined for each of the waters and fractions. The general observed trend was a substantial increase in R_{CT} from the bulk to the < 10 kDa fraction followed by a general decrease in R_{CT} from the < 10 kDa to the < 1 kDa fractions. Like the pseudo first order ozone decay, the large increase in R_{CT} is associated with the removal of the large molecular weight EfOM material.

The molecular weight cutoff of the fractionating process does not reject the inorganic constituents of the water. As such, all inorganic water quality parameters such as alkalinity, pH, and nitrate/nitrite remain constant for each of the fractions in a given water. Because all inorganic characteristics of the water are constant, any changes in system reactivity can be attributed to changes in EfOM characteristics. A simplified model of $HO^{\bullet}$ decay being equal to the difference in $HO^{\bullet}$ formation and scavenging was used to determine the $HO^{\bullet}$ formation of each water and fraction. The model showed the bulk waters to have the highest $HO^{\bullet}$ formation at a time of 30 seconds as well as highest $HO^{\bullet}$ formation for a given ozone exposure. This is attributed to the longer ozone contact time (due to low ozone reactivity) as well as the high scavenging capacity of the water.

From the large increase in ozone reactivity observed from the bulk to the < 10 kDa fraction, it was hypothesized that removing the large molecular weight polysaccharide and cellular debris from the water through conventional coagulation would increase the effectiveness of ozone AOP in micropollutant oxidation. The C2 water was selected for coagulation and a jar test at three different $FeCl_3$ doses was performed. The water with a dose of 16 mg/L was chosen for analysis. Results showed a substantial increase in the k_{O3} and the R_{CT}. SEC was performed on the coagulated sample

and confirmed that a portion of the large molecular weight EfOM had been removed from the system.

Contaminant analysis was performed on the pre ozonated bulk C2 sample as well as the ozonated bulk, coagulated and fractionated samples. Two methods for modeling contaminant removal were employed to predict the expected relative compound removal for each fraction. The first method used the R_{CT} for contaminant removal, the second method used the ozone and $HO^{\bullet}$ exposures to predict contaminant removal. The R_{CT} predicted less contaminant removal than the $HO^{\bullet}$ and ozone exposure model. For compounds that have high reactivity with ozone, both predicted and observed contaminant removal were in very good agreement. The compounds with a more exclusive $HO^{\bullet}$ reactivity had a greater disagreement between predicted and observed contaminant removal. In the case of Meprobamate, the models over predicted contaminant removal but the compound TCEP had greater observed removal than predicted removal. The causes of these discrepancies are unknown.

For the coagulated sample, better contaminant removal was observed when compared to the bulk sample as predicted by both the R_{CT} and the $HO^{\bullet}$ exposures.

6.2: Future Work

Further studies into the affect of coagulation on the ozone AOP process are required to gain a better understanding of how the removal of the large molecular weight material in EfOM increases the reactivity of the system. Process optimization for coagulation with wastewater also needs to be conducted such as studies into the effect of

coagulant type and coagulant dose on EfOM removal, system reactivity and contaminant oxidation.

A more detailed understanding of the relationship between EfOM and ozone reactivity and $HO^{\bullet}$ production/oxidation is required to be able to successfully predict contaminant oxidation. Current models are inaccurate at predicting $HO^{\bullet}$ selective contaminant oxidation.

BIBLIOGRAPHY

Allpike, B. P., A. Heitz, et al. (2005). "Size exclusion chromatography to characterize DOC removal in drinking water treatment." Environmental Science & Technology 39(7): 2334-2342.

Arbuckle, T. E., S. E. Hrudey, et al. (2002). "Assessing exposure in epidemiologic studies to disinfection by-products in drinking water: Report from an international workshop." Environmental Health Perspectives 110: 53-60.

Beltran, J. F. (2004). Ozone Reaction Kinetics for Water and Wastewater Systems. Boca Taton, Lewis Publishers.

Boero, V. J. B., A.R.; Eckenfelder, W.W. (1996). "Molecular weight distribution of soluble microbial products in biological systems." Water Science and Technology 34: 241-248.

Bruce, G. M. P., Richard C.; Snyder, Shane A. (2010). "Toxicological Relevance of Pharmaceuticals in Drinking Water." Environmental Science and Technology 44(14): 5619-5626.

Buffle, M. O., J. Schumacher, et al. (2006). "Ozonation and advanced oxidation of wastewater: Effect of O_3 dose, pH, DOM and HO-scavengers on ozone decomposition and HO generation." Ozone-Science & Engineering 28(4): 247-259.

Buffle, M. O., J. Schumacher, et al. (2006). "Measurement of the initial phase of ozone decomposition in water and wastewater by means of a continuous quench-flow system: Application to disinfection and pharmaceutical oxidation." Water Research 40(9): 1884-1894.

Buffle, M. O. and U. Von Gunten (2006). "Phenols and amine induced HO center dot generation during the initial phase of natural water ozonation." Environmental Science & Technology 40(9): 3057-3063.

Buhler, R. E., J. Staehelin, et al. (1984). "Ozone Decomposition in Water Studied by Pulse-Radiolysis .1. Ho2/O2-and Ho3/O3- as Intermediates." Journal of Physical Chemistry 88(12): 2560-2564.

Buxton, G. V., C. L. Greenstock, et al. (1988). "Critical review of rate constants for reactions of hydrated electrons, hydrogen atom and hydroxyl radicals (·OH/·O-) in aqueous solutions." Journal of Physical and Chemical Reference Data 17: 513-886.

Davis, M. E., R. K. Talukdar, et al. (2007). "Rate Coefficients for the OH + Pinonaldehyde (C10H16O2) Reaction between 297 and 374 K." Environ. Sci. Technol. 41(11): 3959-3965.

Dong, M. M. M., Stephen P.; Rosario-Ortiz, Fernando L. (2010). "Reactivity of Effluent Organic Matter (EfOM) with Hydroxyl Radical as a Function of Molecular Weight." Environmental Science and Technology 44(15): 5714-5720.

Elovitz, M. S. and U. von Gunten (1999). "Hydroxyl radical ozone ratios during ozonation processes. I-The R-ct concept." Ozone-Science & Engineering 21(3): 239-260.

Esplugas, S., D. M. Bila, et al. (2007). "Ozonation and advanced oxidation technologies to remove endocrine disrupting chemicals (EDCs) and pharmaceuticals and

personal care products (PPCPs) in water effluents." Journal of Hazardous Materials 149: 631-642.
Fonseca, A. C., R. S. Summers, et al. (2007). "Extra-Cellular Polysaccharides, Soluble Microbial Products, and Natural Organic Matter Impact on Nanofiltration Membranes Flux Decline." Environmental Science & Technology 41(7): 2491-2497.
Her, N., G. Amy, et al. (2002). "Optimization of method for detecting and characterizing NOM by HPLC-size exclusion chromatography with UV and on-line DOC detection." Environmental Science & Technology 36(5): 1069-1076.
Her, N., Amy, G., McKnight, D., Sohn, J. and Yoon, Y. (2003). "Characterization of DOM as a function of MW by fluorescence EEM and HPLC-SEC using UVA, DOC, and fluorescence detection." Water Research 37: 4295-4303.
Hickel, B. S., K. (1992). "Reaction of hydroxyl radicals with ammonia in liquid water at elevated temperatures." Radiat Phys Chem 39: 355-357.
Hoigne, J. (1998). Chemistry of aqueous ozone and transformation of pollutants by ozonation and advanced ozidation processes. Berlin, Springer.
Hollender, J. Z., Saskia; Kiepke, Stephan; Krauss, Martin; Mcardell, Christa; Ort, Christoph; Singer, Heinz; Von Gunten, Urs; Siegrist, Hanstruedi (2009). "Elimination of Organic Micropollutants in a Municipal Wastewater Treatment Plant Upgraded with a Full-Scale Post-Ozonation Followed by Sand Filtration." Environmental Science and Technology 43: 7862-7869.
Huber, M. M., S. Canonica, et al. (2003). "Oxidation of pharmaceuticals during ozonation and advanced oxidation processes." Environmental Science & Technology 37(5): 1016-1024.
Jarusutthirak, C. and G. Amy (2007). "Understanding soluble microbial products (SMP) as a component of effluent organic matter (EfOM)." Water Research 41(12): 2787-2793.
Jiang, T. K., M.; De Schepper, V.; Nam Nam, S.; Nopens, I.; Vanrolleghem, P.; Amy, G. (2010). "Characterization of Soluble Microbial Products and Their Fouling Impacts in Membrane Bioreactors." Environmental Science and Technology 44: 6642-6648.
Jobling, S., M. Nolan, et al. (1998). "Widespread sexual disruption in wild fish." Environmental Science & Technology 32(17): 2498-2506.
Jobling, S. R., T.; White, R.; Parker, M. G.; Sumpter, J. P. (1995). "A Variety of Environmentally Persistent Chemicals, Including Some Phthalate Plasticizers, Are Weakly Estrogenic." Environmental Health Perspectives 103(6): 582-587.
Krasner, S. W., J. P. Croue, et al. (1996). "Three approaches for characterizing NOM." Journal American Water Works Association 88(6): 66-79.
Logager, T. S., K. (1993). "Formation and decay of peroxynitrous acid - a pulse radiolysis study." Journal of Physical Chemistry 97: 6664-6669.
McKnight D.M, B. E. W., Westerhoff P.K., Doran P.T, Anderson D.T (2001). "Spectrofluorometric characterization of dissolved organic matter for identification of precursor organic material and aromaticity." Luminol. Oceanogr. 46: 38-48.
Mvula, E. N., Sergej; Von Sonntag, Clemmens (2009). "Ozonolysis of Lignin Models in Aqueous Solution; Anisole, 1,2-Dimethoxybenzene, 1,4-Dimethoxybenzene, and

1,3,5-Trimethoxybenzene." Environmental Science and Technology 43(16): 6275-6282.
Nam, S.-N., S. W. Krasner, et al. (2008). "Differentiating effluent organic matter (EfOM) from natural organic matter (NOM): Impact of EfOM on drinking water sources." Advanced Environmental Monitoring: 259-270.
Namkung, E. and B. E. Rittmann (1986). "Soluble Microbial Products (Smp) Formation Kinetics by Biofilms." Water Research 20(6): 795-806.
Pribyl, M. T. F. W., P.A.; Wanner, J. (1997). "Amount and nature of soluble refractory organics produced by activated sludge microorganisms in sequencing batch and continuous flow reactors." Water Science and Technology 35(1): 27-34.
Rosario-Ortiz, F. L., Al-Samarrai, H. A., Kozawa, K., Gerringer, F. W., Gabelich, C. J. and Suffet, I. H. (2004). "Characterization of the polarity of natural organic matter using solid phase extraction." In Proceedings of the XII International meeting of the IHSS, Sao Pedro, Brazil, July 2004: 722-724.
Rosario-Ortiz, F. L., S. P. Mezyk, et al. (2008). "Quantitative correlation of absolute hydroxyl radical rate constants with non-isolated effluent organic matter bulk properties in water." Environmental Science & Technology 42(16): 5924-5930.
Rosario-Ortiz, F. L., S. P. Mezyk, et al. (2008). "Effect of oxidation on the molecular and kinetic properties of effluent organic matter." Journal of Applied Oxidation Technologies 11(3): 529-535.
Rosenfeldt, E. J. and K. G. Linden (2004). "Comparative Efficiency of OH Radical Formation by Ozone and UV Processes: Impact for Contaminant Treatment." Proceedings of the 2004 AWWA WQTC Conference.
Rosenfeldt, E. J. and K. G. Linden (2004). "Degradation of endocrine disrupting chemicals bisphenol A, ethinyl estradiol, and estradiol during UV photolysis and advanced oxidation processes." Environmental Science & Technology 38(20): 5476-5483.
Rosenfeldt, E. J., K. G. Linden, et al. (2006). "Comparison of the efficiency of OH radical formation during ozonation and the advanced oxidation processes O_3/H_2O_2 and UV/H_2O_2." Water Research 40: 3695-3704.
Ruiz-Haas, P., K. D. Cho, et al. UV and Advanced Oxidaiton Treatment Based Technologies for Removal of Chemical Pollutants for Water Reuse: 1-7.
Snyder, S., B. Vanderford, et al. (2003). "Analytical methods used to measure endocrine disrupting compounds in water." Practice Periodical of Hazardous, Toxic, and Radioactive Waste Management October 2003: 224-234.
Snyder, S., P. Westerhoff, et al. (2003). "Pharmaceuticals, personal care products, and endocrine disruptors in water: Implications for the water industry." Environment Engineering Science 20(5): 449-469.
Snyder, S. A., S. Adham, et al. (2007). "Role of membranes and activated carbon in the removal of endocrine disruptors and pharmaceuticals." Desalination 202(1-3): 156-181.
Song, G. W., J.; Chiu, C.; Westerhoff, P. (2010). "Biogenic Nanoscale Colloids in Wastewater Effluents." Environmental Science and Technology 44(21): 8216-8222.
Sonntag, C. v. and H.-P. Schuchmann (1994). "Pulse Radiolysis." Methods in Enzymology 233: 3-20.

Staehelin, J., R. E. Buhler, et al. (1984). "Ozone Decomposition in Water Studied by Pulse-Radiolysis .2. Oh and Ho4 as Chain Intermediates." Journal of Physical Chemistry 88(24): 5999-6004.

Staehelin, J. and J. Hoigne (1982). "Decomposition Of Ozone In Water - Rate Of Initiation By Hydroxide Ions And Hydrogen-Peroxide." Environmental Science & Technology 16(10): 676-681.

Tomiyasu, H., Fukutomi H., et al. (1985). "Kinetics and Mechanism of Ozone Decomposition in Basic Aqueous-Solution." Inorganic Chemistry 24(19): 2962-2966.

Trenholm et al., 2009 R.A. Trenholm, B.J. Vanderford and S.A. Snyder, On-line SPE LC-MS/MS analysis of pharmaceutical indicators in water: a green alternative to conventional methods, *Talanta* **79** (2009), pp. 1425–1432

von Gunten, U. (2003). "Ozonation of drinking water: Part I. Oxidation kinetics and product formation." Water Research 37(7): 1443-1467.

von Gunten, U. (2007). "The basics of oxidants in water treatment. Part B: ozone reactions." Water Science and Technology 55(12): 25-9.

Weiss, J. (1935). "Investigations on the radical HO2 in solution." Trans. Faraday Soc. 31: 668-681.

Wert, E. C., F. L. Rosario-Ortiz, et al. (2009). "Effect of ozone exposure on the oxidation of trace organic contaminants in wastewater." Water Research 43: 1005-1014.

Whitham, K., S. Lyons, et al. (1995). Linear accelerator for radiation chemistry research at Notre Dame. IEEE Proceedings Particle Accelerator Conference and International Conference on High Energy Accelerators, Dallas, Texas.